Supplementary Information

(1*E*)-1,2-Diaryldiazene Derivatives Containing a Donor–π-Acceptor-Type Tolane Skeleton as Smectic Liquid–Crystalline Dyes

Shigeyuki Yamada [1,*], Keigo Yoshida [1], Yuto Eguchi [1], Mitsuo Hara [2,3], Motohiro Yasui [1] and Tsutomu Konno [1]

[1] Faculty of Molecular Chemistry and Engineering, Kyoto Institute of Technology, Matsugasaki, Sakyo-ku, Kyoto 606-8585, Japan; m2673040@edu.kit.ac.jp (K.Y.); b0151021@edu.kit.ac.jp (Y.E.); myasui@kit.ac.jp (M.Y.); konno@kit.ac.jp (T.K.)
[2] Department of Molecular and Macromolecular Chemistry, Graduate School of Engineering, Nagoya University, Furo-cho, Chikusa-ku, Nagoya 464-8603, Japan; mhara@chembio.nagoya-u.ac.jp
[3] Faculty of Engineering and Design, Kagawa University, 2217-20, Hayashi-cho, Takamatsu 761-0396, Japan
* Correspondence: syamada@kit.ac.jp

Table of Contents

Experimental

General method

^{1}H nuclear magnetic resonance (NMR) (400 MHz) and ^{13}C NMR (100 MHz) spectra were acquired using an AVANCE III 400 NMR spectrometer (Bruker, Rheinstetten, Germany) in a chloroform-*d* ($CDCl_3$) solution, and chemical shifts were reported in parts per million (ppm) based on the residual protons or carbon in the NMR solvent. ^{19}F NMR (376 MHz) spectra were acquired using an AVANCE III 400 NMR spectrometer (Bruker, Rheinstetten, Germany) in $CDCl_3$ solution with $CFCl_3$ (δ_F = 0 ppm) or C_6F_6 (δ_F = −163 ppm) as an internal standard. Infrared (IR) spectra were recorded using the KBr method on an FTIR-4100 type A spectrometer (JASCO, Tokyo, Japan). All IR spectra are reported in wavenumber (cm^{-1}) units. High-resolution mass spectra (HRMS) were recorded on a JMS700MS spectrometer (JEOL, Tokyo, Japan) using the fast atom bombardment (FAB) method. Before use, all chemicals were reagent-grade and purified using standard methods. Melting temperature (T_m) was measured using a DSC-60 differential scanning calorimeter (SHIMADZU, Kyoto, Japan) under a nitrogen atmosphere at a scan rate of 5 °C min^{-1}. The progress of the reaction was monitored by thin-layer chromatography (TLC) on silica gel TLC plates (Merck, Silica Gel, $60F_{254}$; New Jersey, NJ, USA). Column chromatography was performed using silica gel (FUJIFILM Wako Pure Chemical Corporation, Wako-gel® 60 N, 38 μm to 100 μm; Osaka, Japan).

Typical synthetic procedure for 4-amino-4'-decyloxydiphenylacetylene (3a)

In a two-necked round-bottomed flask, equipped with a Teflon®-coated stirring bar, was placed 4-decyloxy-1-iodobenzene (3.24 g, 9.0 mmol), $Cl_2Pd(PPh_3)_2$ (0.32 g, 0.45 mmol), PPh_3 (0.12 g, 0.45 mmol), Et_3N (2.5 mL) and THF (35 mL). To the solution was added CuI (0.17 g, 0.90 mmol) and 4-ethynylaniline (1.26 g, 11 mmol), and the solution was stirred at 80 °C for 18 h. After being stirred for 18 h, precipitate formed during the reaction was separated by atmospheric filtration, and the filtrate was poured into saturated aqueous NH_4Cl solution. The crude product was extracted with Et_2O (50 mL) three times. The combined organic layer was dried over anhydrous sodium sulfate (Na_2SO_4), filtered under atmospheric pressure, and evaporated under reduced pressure using a rotary evaporator. The residue was subjected to silica-gel column chromatography using hexane/CH_2Cl_2 1/1 (v/v) mixed solvent as an eluent, followed by recrystallization from $CHCl_3$/hexane (v/v = 1/1), producing the coupling product **3a** in 40% (1.26 g, 3.6 mmol) as a white solid.

4-Amino-4'-decyloxydiphenylacetylene (3a)

Yield: 40% (white solid); T_m: 87–88 °C (observed by POM); ^{1}H NMR ($CDCl_3$): *d* 0.88 (t, J = 7.2 Hz, 3H), 1.23–1.38 (m, 10H), 1.45 (quin, J = 7.2 Hz, 2H), 1.78 (quin, J = 6.8 Hz, 2H), 3.79 (brs, 2H), 3.95 (t, J = 6.8 Hz, 2H), 6.63 (d, J = 8.4 Hz, 2H), 6.84 (d, J = 8.8 Hz, 2H), 7.31 (d, J = 8.4 Hz, 2H), 7.41 (d, J = 8.8 Hz, 2H); ^{13}C NMR ($CDCl_3$): *d* 14.1, 22.7, 26.0, 29.2, 29.3, 29.4, 29.5, 29.6, 31.9, 68.0, 87.2, 88.4, 113.0, 114.4, 114.7, 115.7, 132.70, 132.73, 146.3, 158.8; IR (KBr): *n* 3468, 3030, 2953, 2881, 1609, 1518, 1320, 1246, 1190, 1040, 947, 834 cm^{-1}; HRMS (FAB) Calcd for (M^+) $C_{24}H_{31}NO$: 349.2406, Found: 3492412.

4-Amino-4'-(7,7,8,8,9,9,10,10,10-nonafluorodecyloxy)diphenylacetylene (3b)

Yield: 50% (white solid); T_m: 124–125 °C (observed by POM); ^{1}H NMR ($CDCl_3$): *d* 1.41–1.59 (m, 4H), 1.65 (quin, J = 7.6 Hz, 2H), 1.81 (quin, J = 6.8 Hz, 2H), 1.99–2.15 (m, 2H), 3.79 (brs, 2H), 3.97 (t, J = 6.8 Hz, 2H), 6.63 (d, J = 8.8 Hz, 2H), 6.84 (d, J = 8.8 Hz, 2H), 7.31 (d, J = 8.8 Hz, 2H), 7.42 (d, J = 8.8 Hz, 2H); ^{13}C NMR ($CDCl_3$): *d* 20.1,

25.7, 28.8, 29.0, 30.7 (t, J = 22.0 Hz), 67.7, 87.2, 88.5, 113.0, 114.4, 114.8, 115.9, 132.7, 132.8, 146.3, 158.6, and the four signals that should be assigned to C_4F_9 are split by the F atoms, and their intensities are too low for accurate assignment; ^{19}F NMR ($CDCl_3$, C_6F_6): *d* –82.33 (t, J = 9.4 Hz, 3F), –115.80 to –116.08 (m, 2F), –125.71 to –125.89 (m, 2F), –127.28 to –127.46 (m, 2F); IR (KBr): *n* 3344, 2943, 2867, 1609, 1519, 1319, 1284, 1247, 1133, 1046, 839 cm^{-1}; HRMS (FAB) Calcd for (M^+) $C_{24}H_{22}F_9NO$: 511.1558, Found: 511.1557.

4-Amino-4'-(5,5,6,67,7,8,8,9,9,10,10,10-tridecafluorodecyloxy)diphenylacetylene (3c)

Yield: 13% (white solid); T_m: 158–160 °C (observed by POM); ^1H NMR ($CDCl_3$): *d* 1.78–1.93 (m, 4H), 2.08–2.26 (m, 2H), 3.79 (brs, 2H), 4.01 (t, J = 6.0 Hz, 2H), 6.63 (d, J = 8.8 Hz, 2H), 6.84 (d, J = 8.8 Hz, 2H), 7.31 (d, J = 8.8 Hz, 2H), 7.42 (d, J = 8.8 Hz, 2H); ^{13}C NMR ($CDCl_3$): *d* 17.3, 28.7, 30.7 (t, J = 22.0 Hz), 67.2, 88.6, 97.2, 113.0, 114.4, 114.8, 117.2, 132.8, 137.9, 146.4, 158.4, and the six signals that should be assigned to C_6F_{13} are split by the F atoms, and their intensities are too low for accurate assignment; ^{19}F NMR ($CDCl_3$, C_6F_6): *d* –82.06 (t, J = 9.8 Hz, 3F), –115.60 to –115.86 (m, 2F), –123.09 to –123.36 (m, 2F), –124.06 to –124.25 (m, 2F), –124.74 to –124.92 (m, 2F), –127.37 to –127.52 (m, 2F); IR (KBr): *n* 3343, 3033, 2954, 2850, 2212, 1608, 1518, 1475, 1319, 1249, 1172, 1024, 997, 841 cm^{-1}; HRMS (FAB) Calcd for (M^+) $C_{24}H_{18}F_{13}NO$: 583.1181, Found: 583.1191.

NMR spectrum

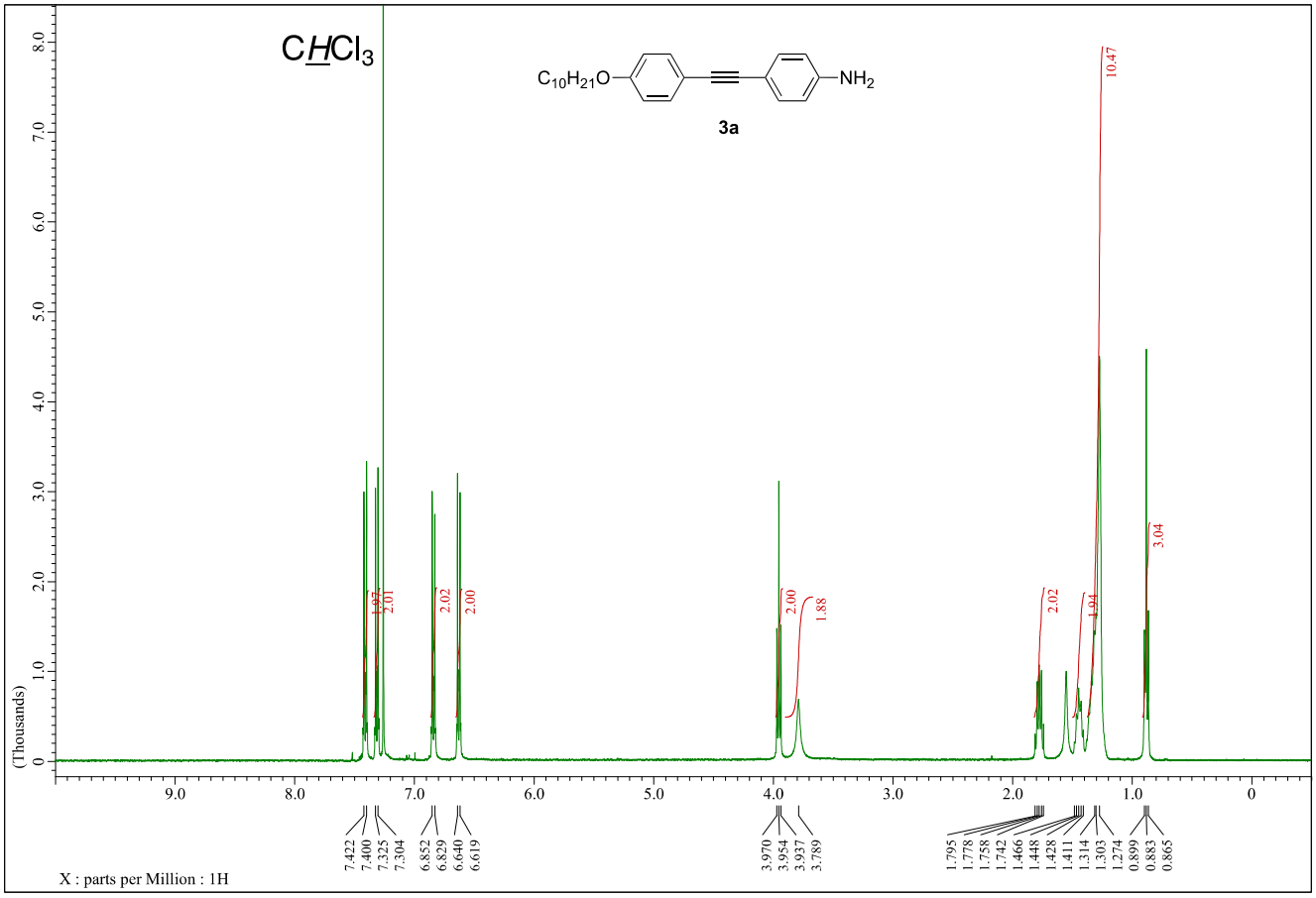

Figure S1. ^{1}H NMR spectrum of **3a** (400 MHz, $CDCl_3$)

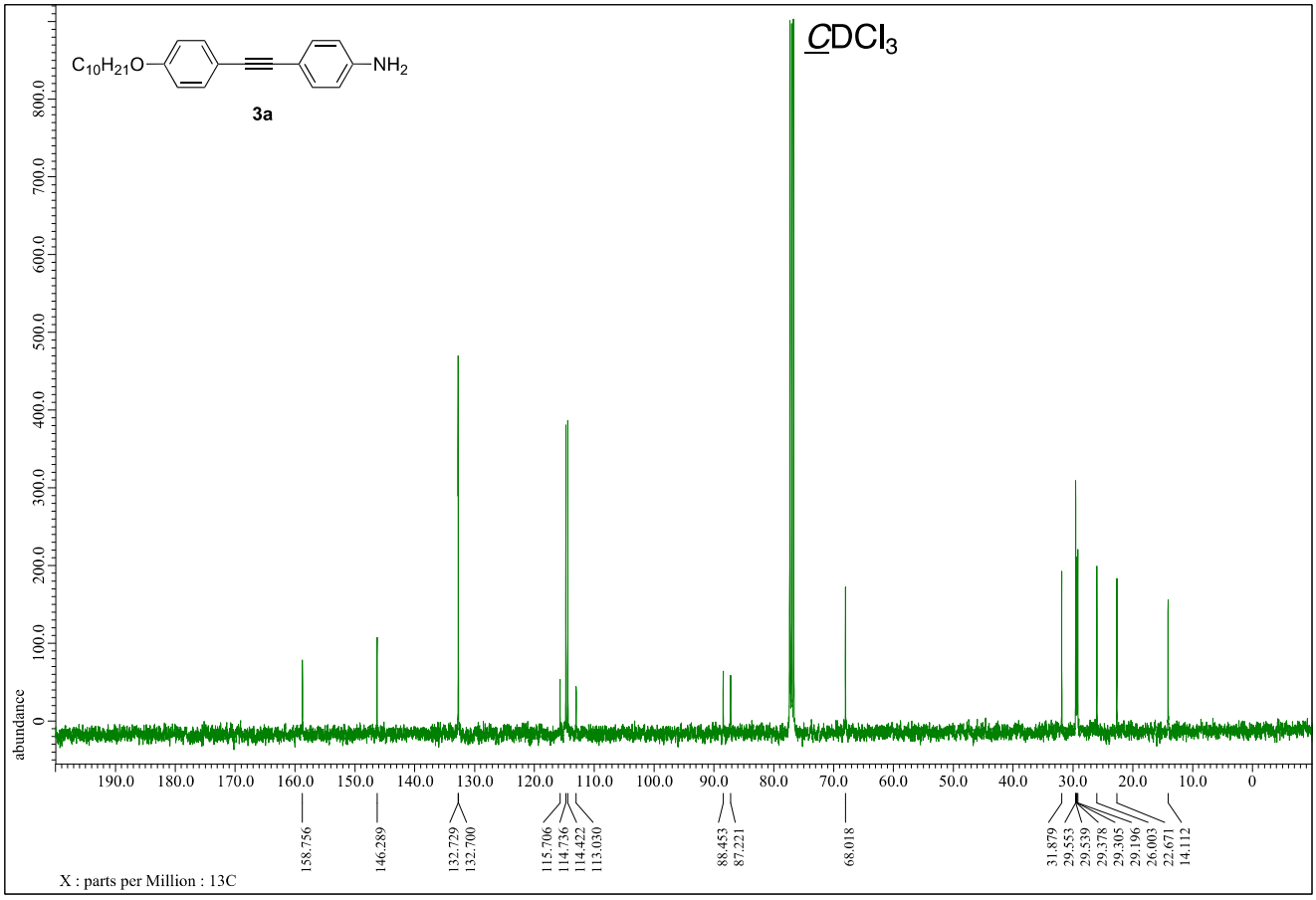

Figure S2. ^{13}C NMR spectrum of **3a** (100 MHz, $CDCl_3$)

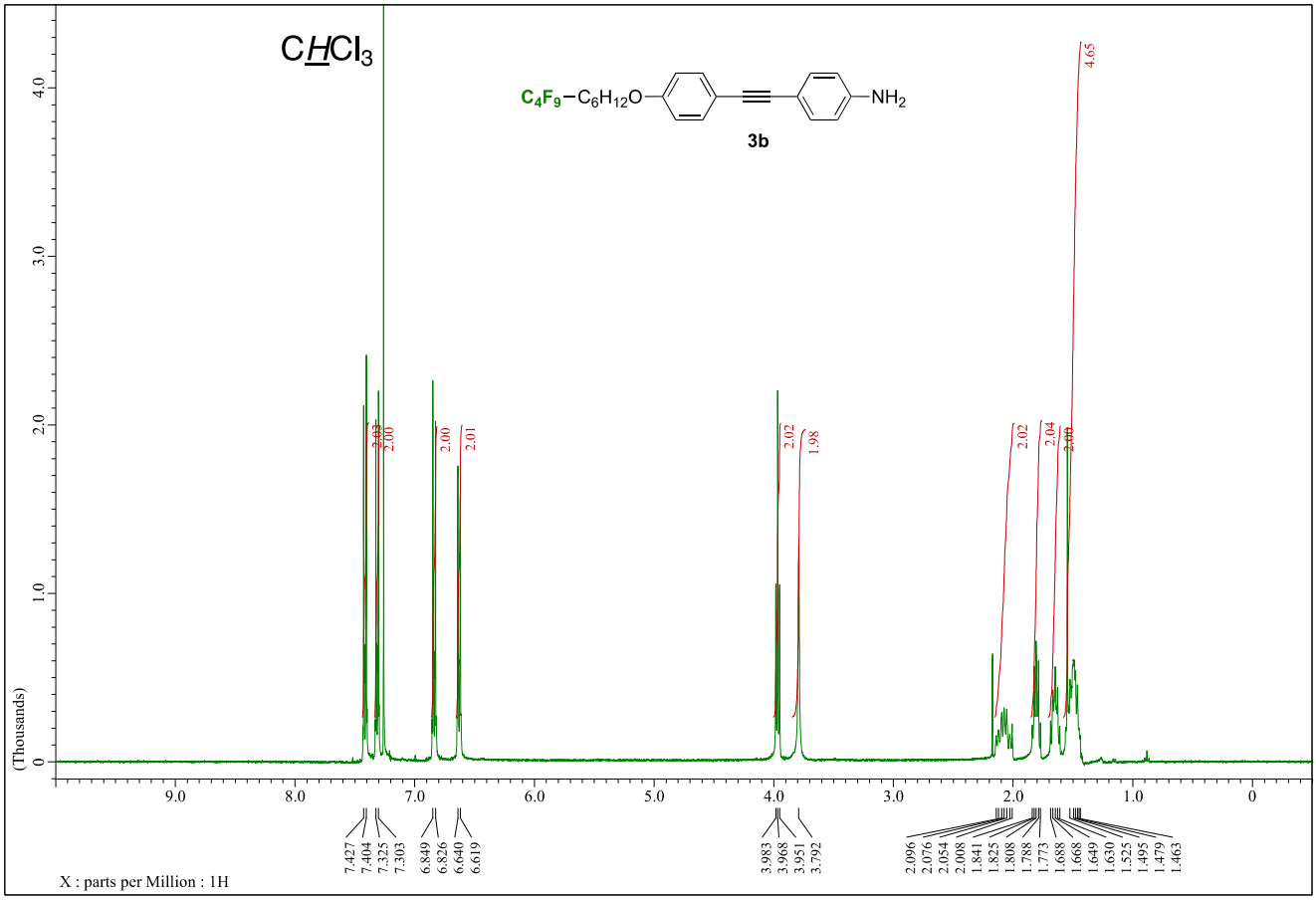

Figure S3. ^{1}H NMR spectrum of **3b** (400 MHz, $CDCl_3$)

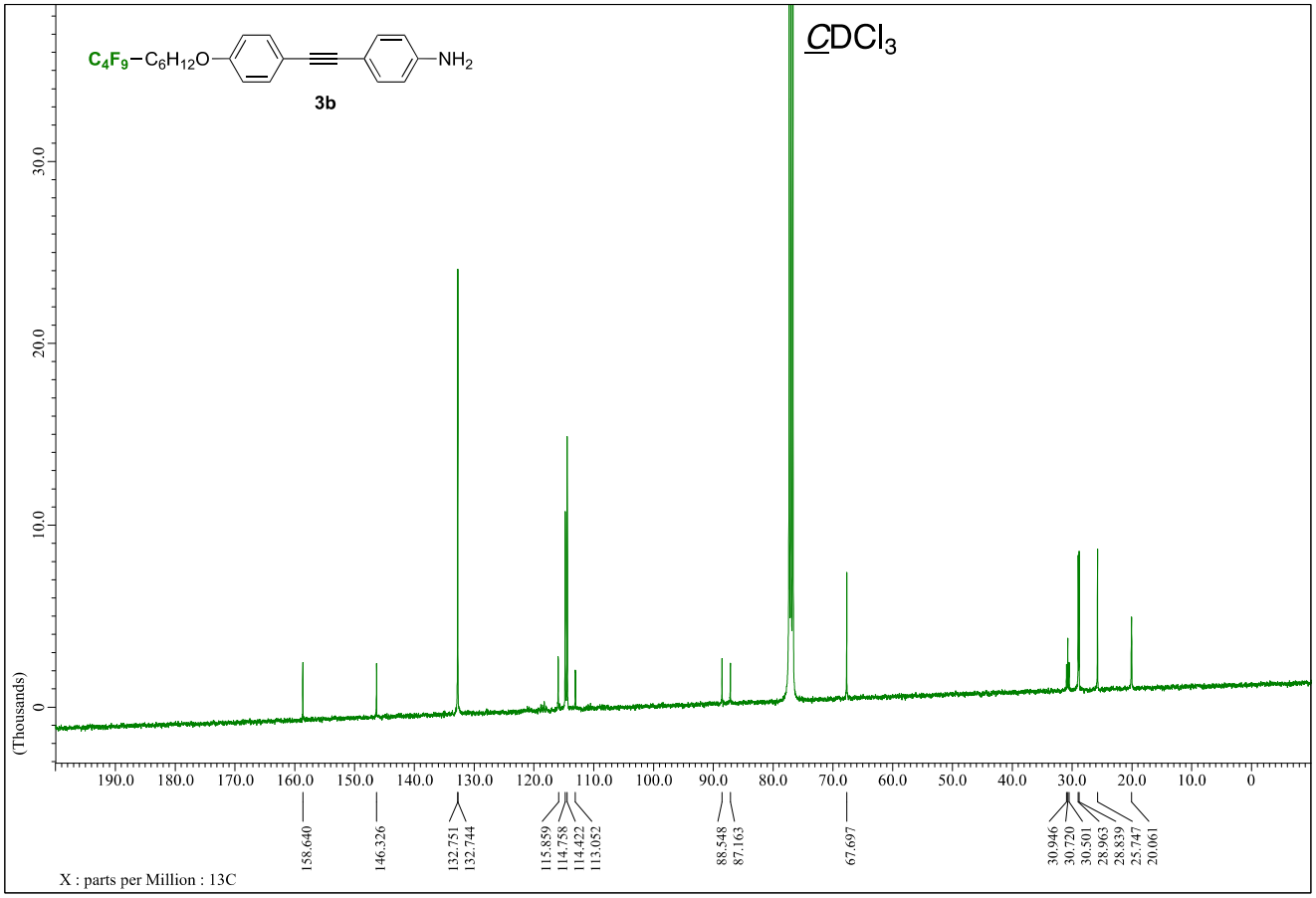

Figure S4. ^{13}C NMR spectrum of **3b** (100 MHz, $CDCl_3$)

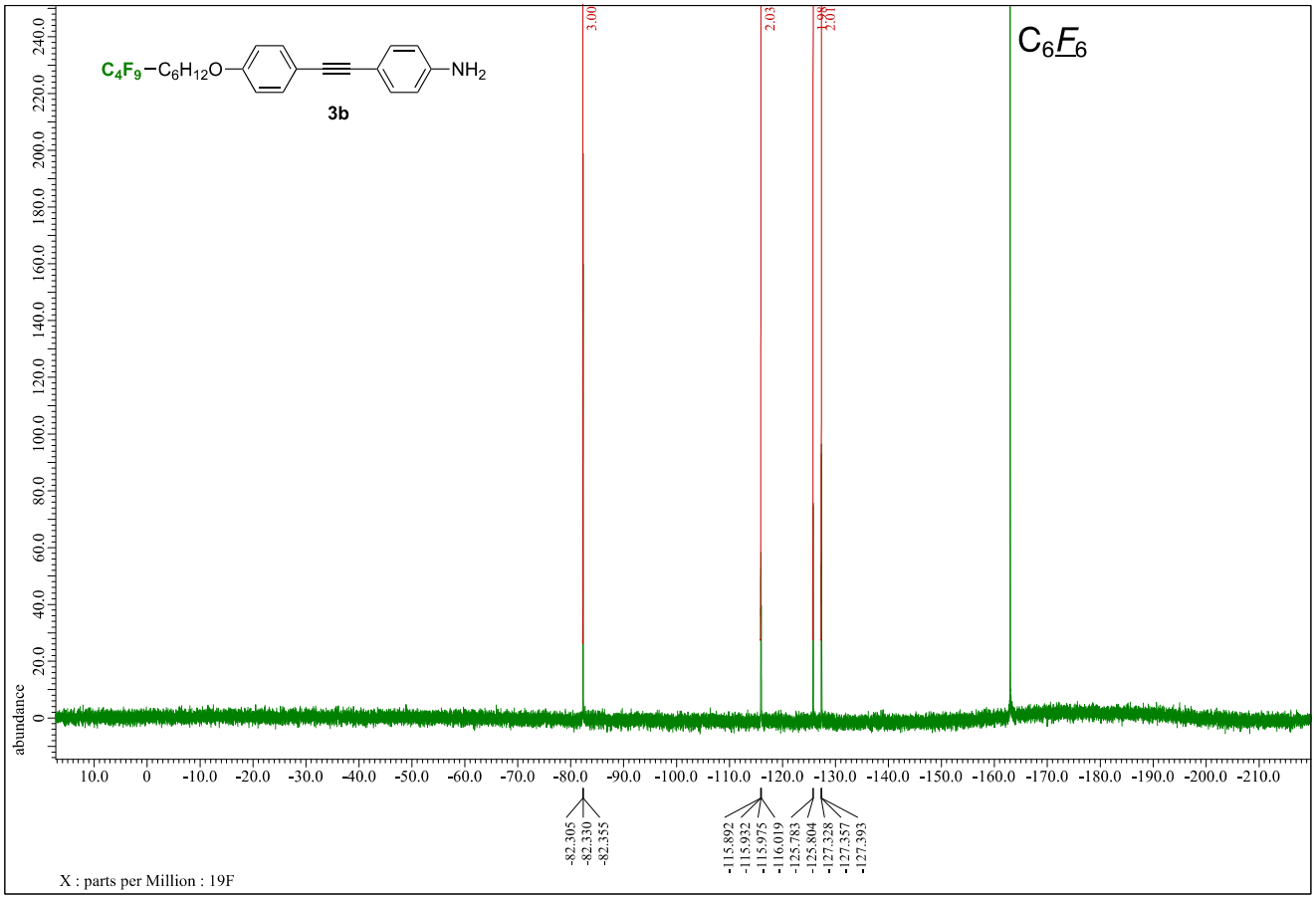

Figure S5. ^{19}F NMR spectrum of **3b** (376 MHz, $CDCl_3$, C_6F_6)

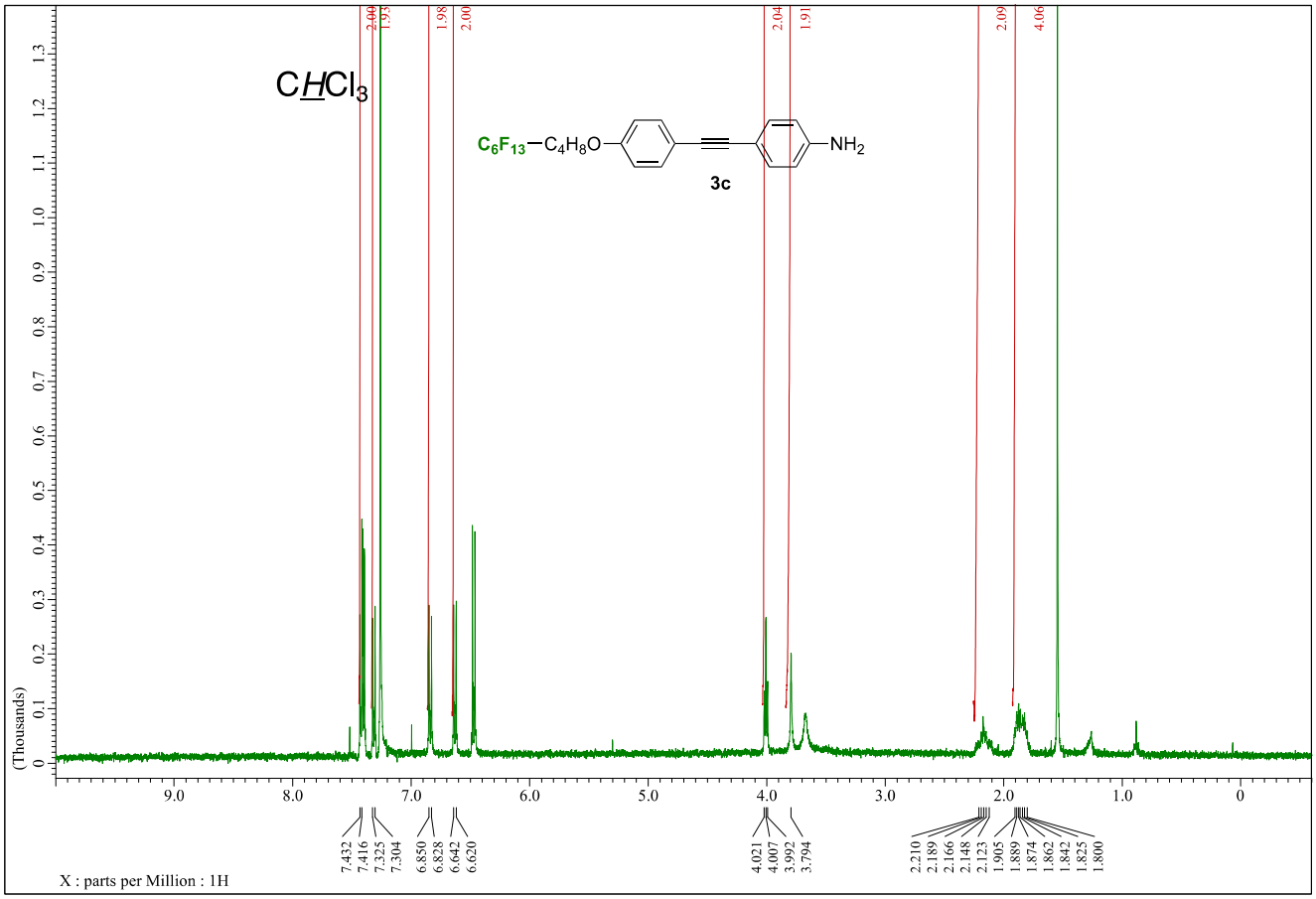

Figure S6. ^{1}H NMR spectrum of **3c** (400 MHz, $CDCl_3$)

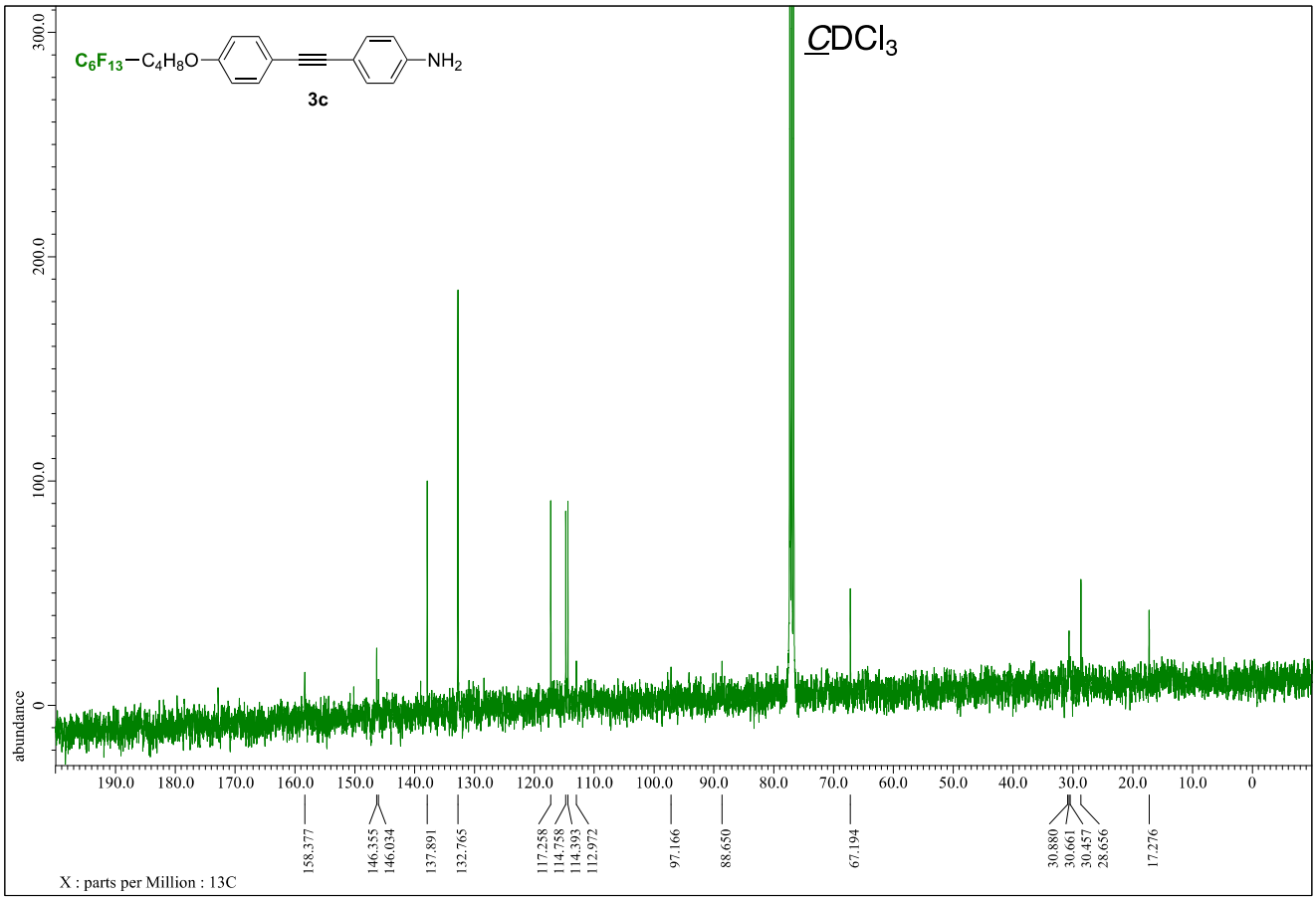

Figure S7. ^{13}C NMR spectrum of **3c** (100 MHz, $CDCl_3$)

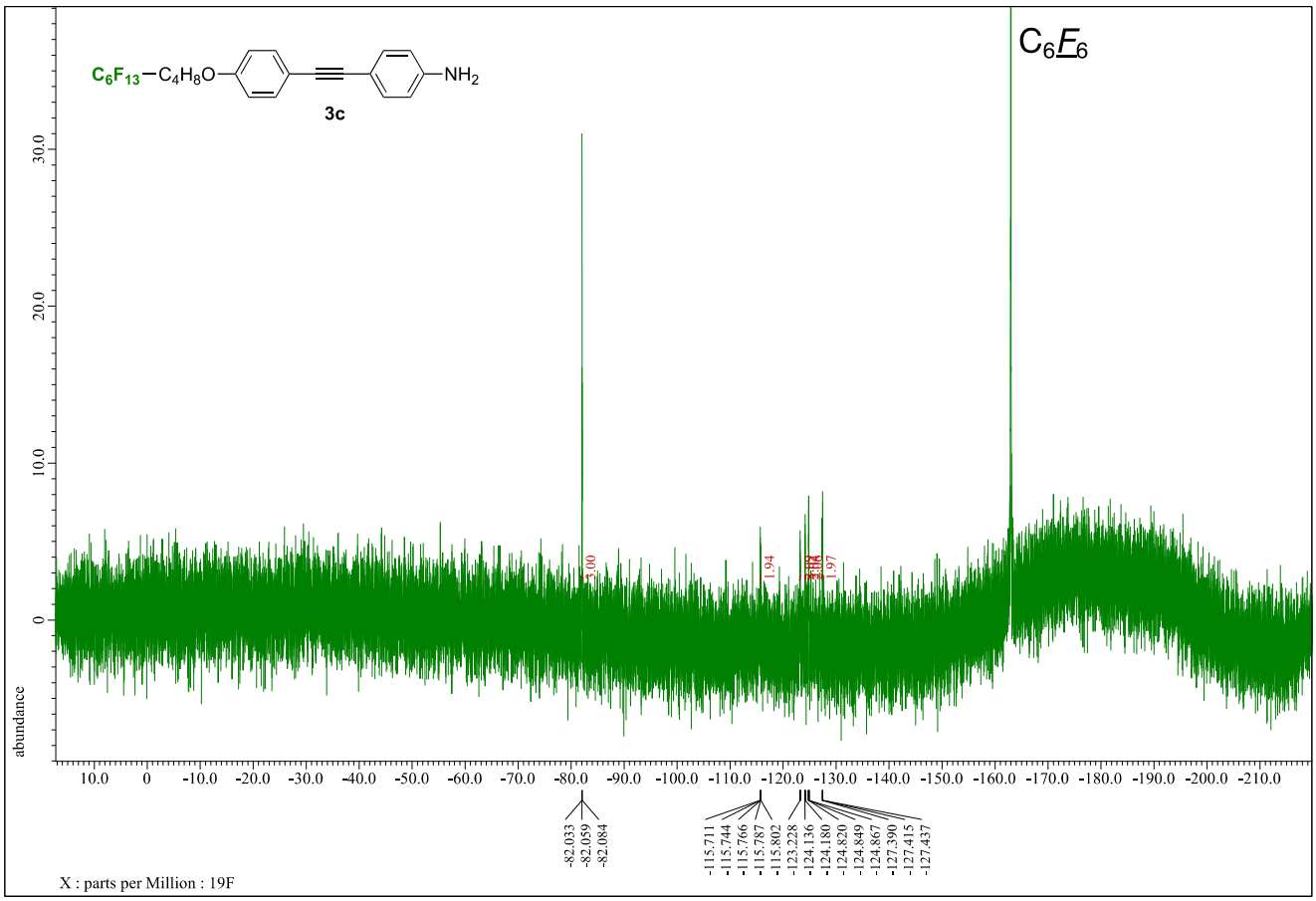

Figure S8. ^{19}F NMR spectrum of **3c** (376 MHz, $CDCl_3$, C_6F_6

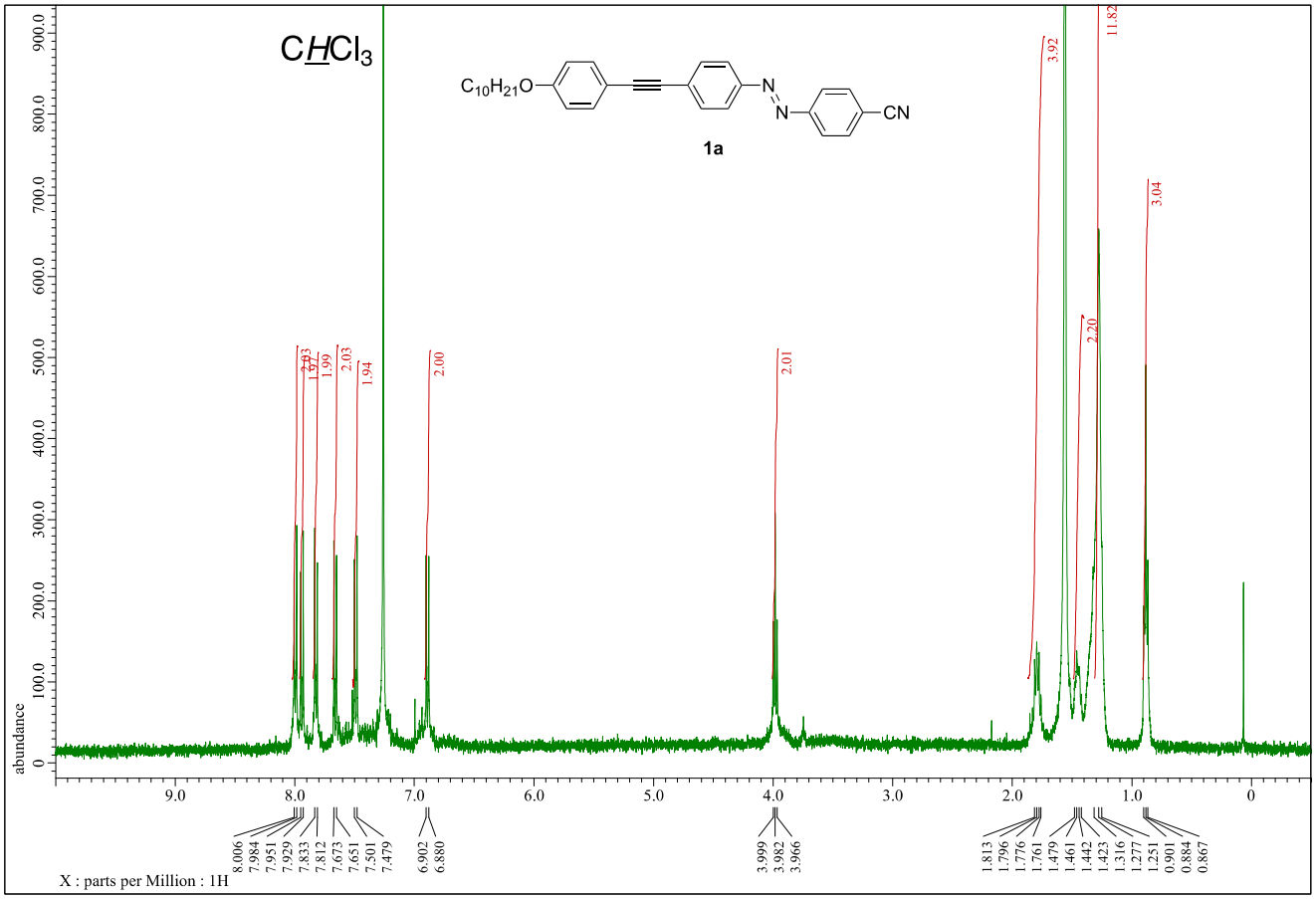

Figure S9. ^{1}H NMR spectrum of **1a** (400 MHz, $CDCl_3$)

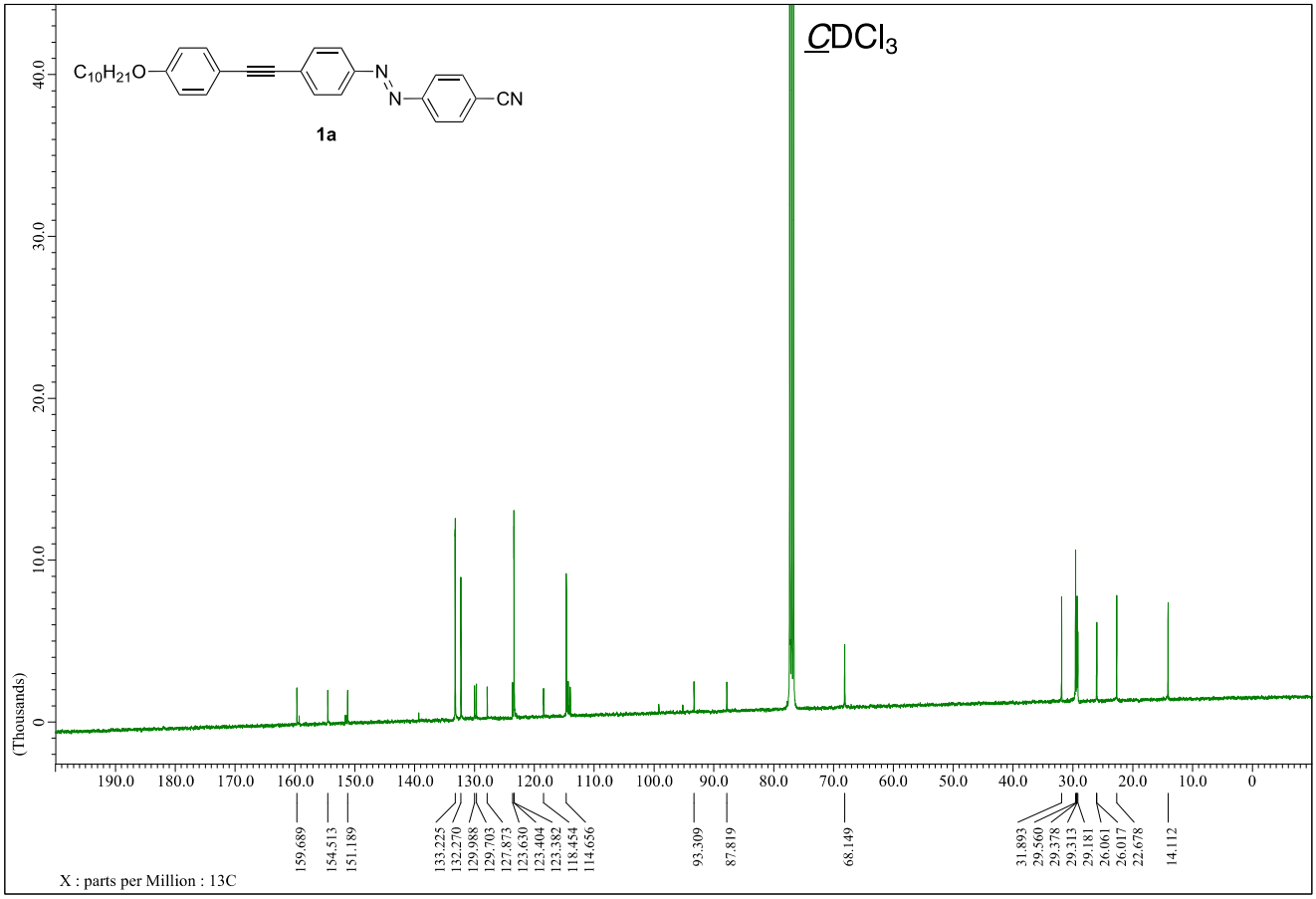

Figure S10. ^{13}C NMR spectrum of **1a** (100 MHz, $CDCl_3$)

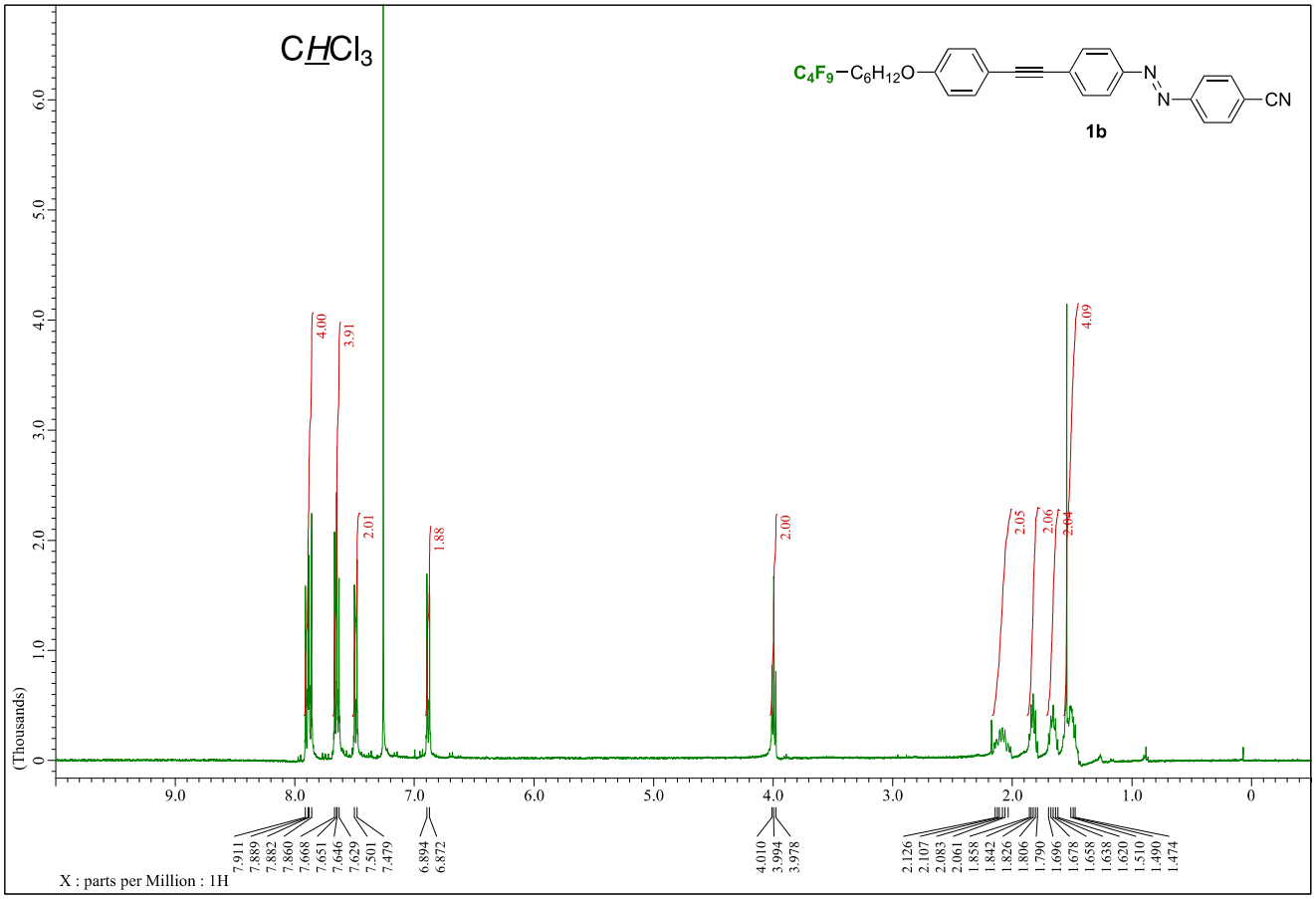

Figure S11. ^{1}H NMR spectrum of **1b** (400 MHz, $CDCl_3$)

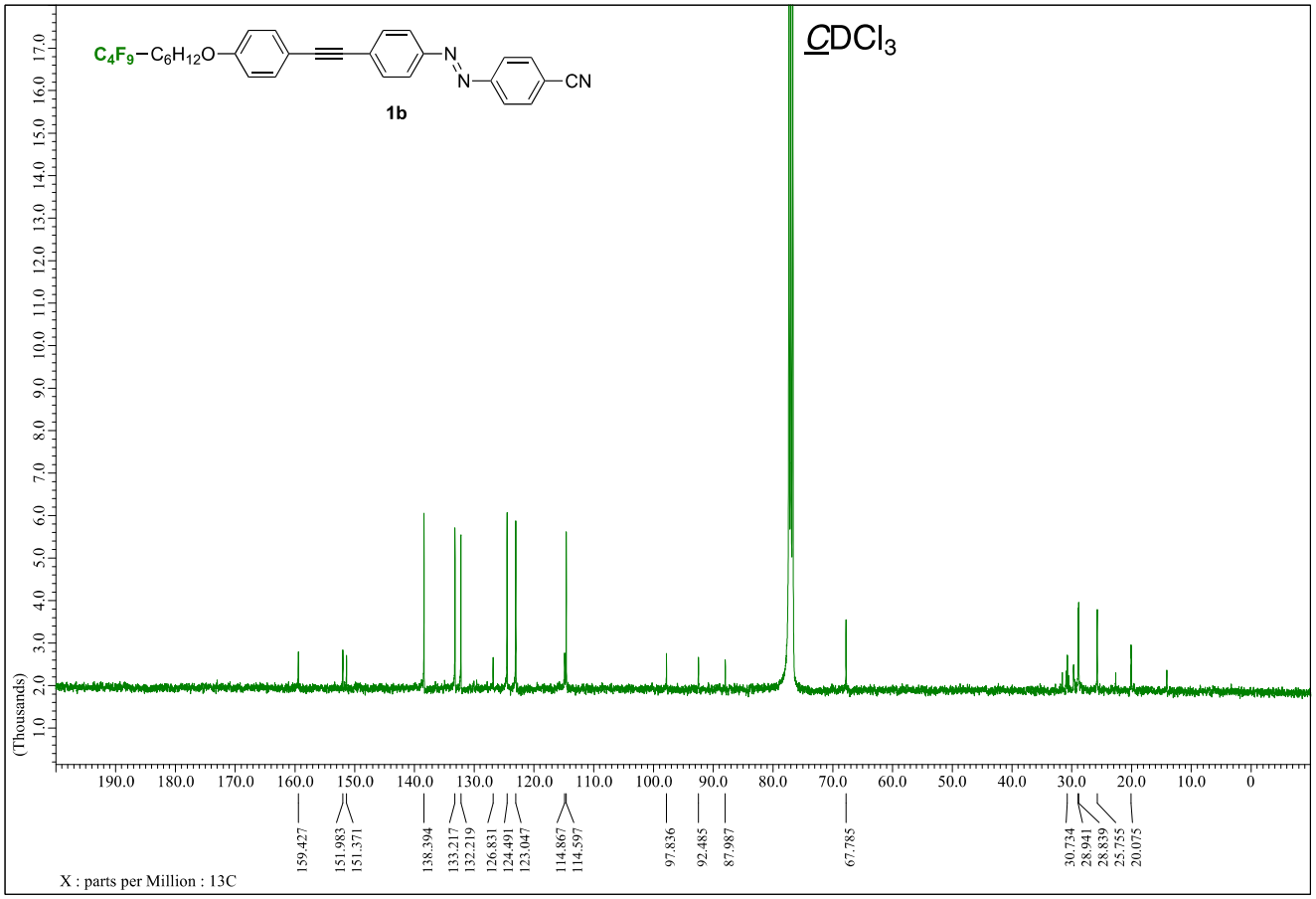

Figure S12. ^{13}C NMR spectrum of **1b** (100 MHz, $CDCl_3$)

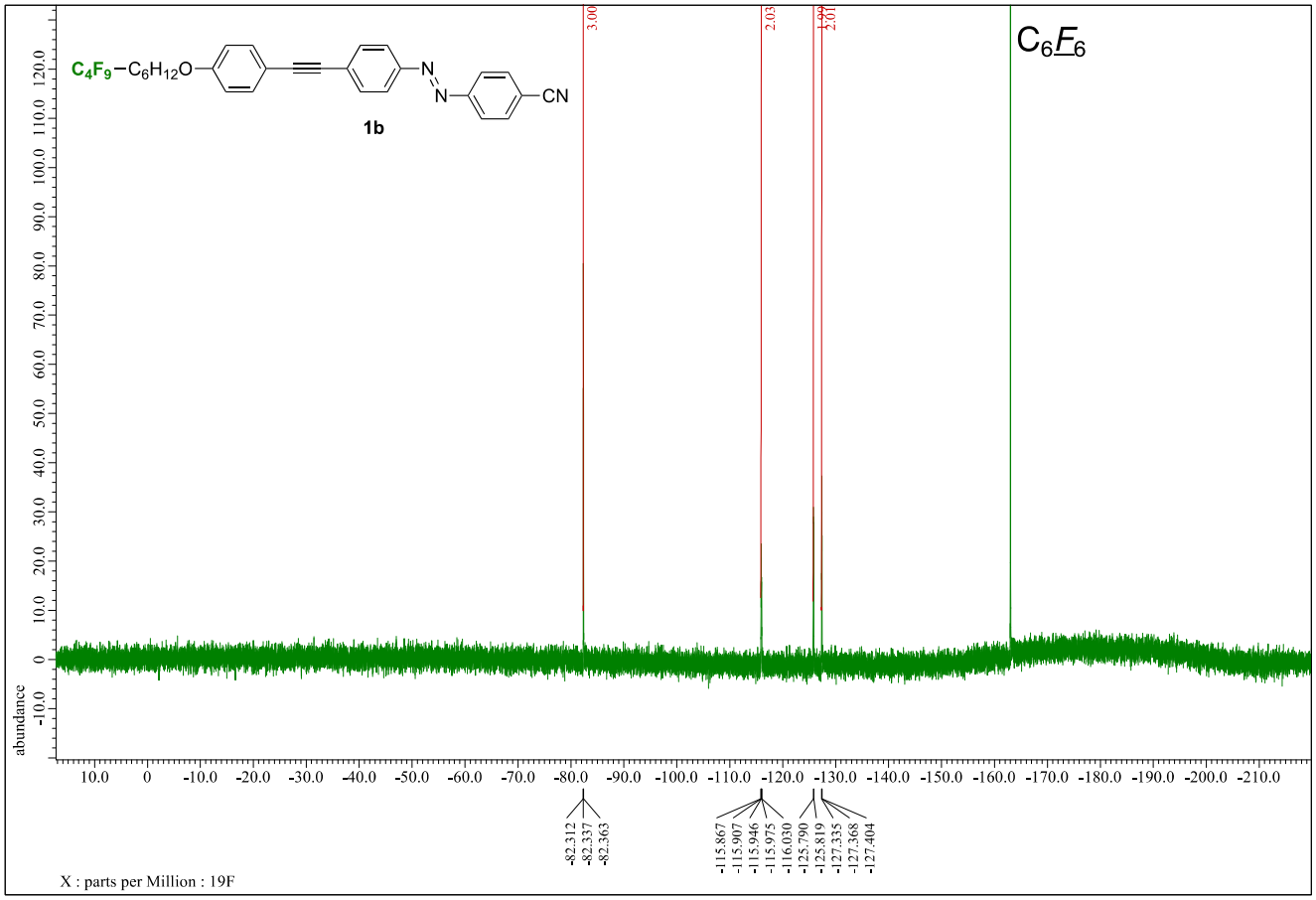

Figure S13. ^{19}F NMR spectrum of **1b** (376 MHz, $CDCl_3$, C_6F_6)

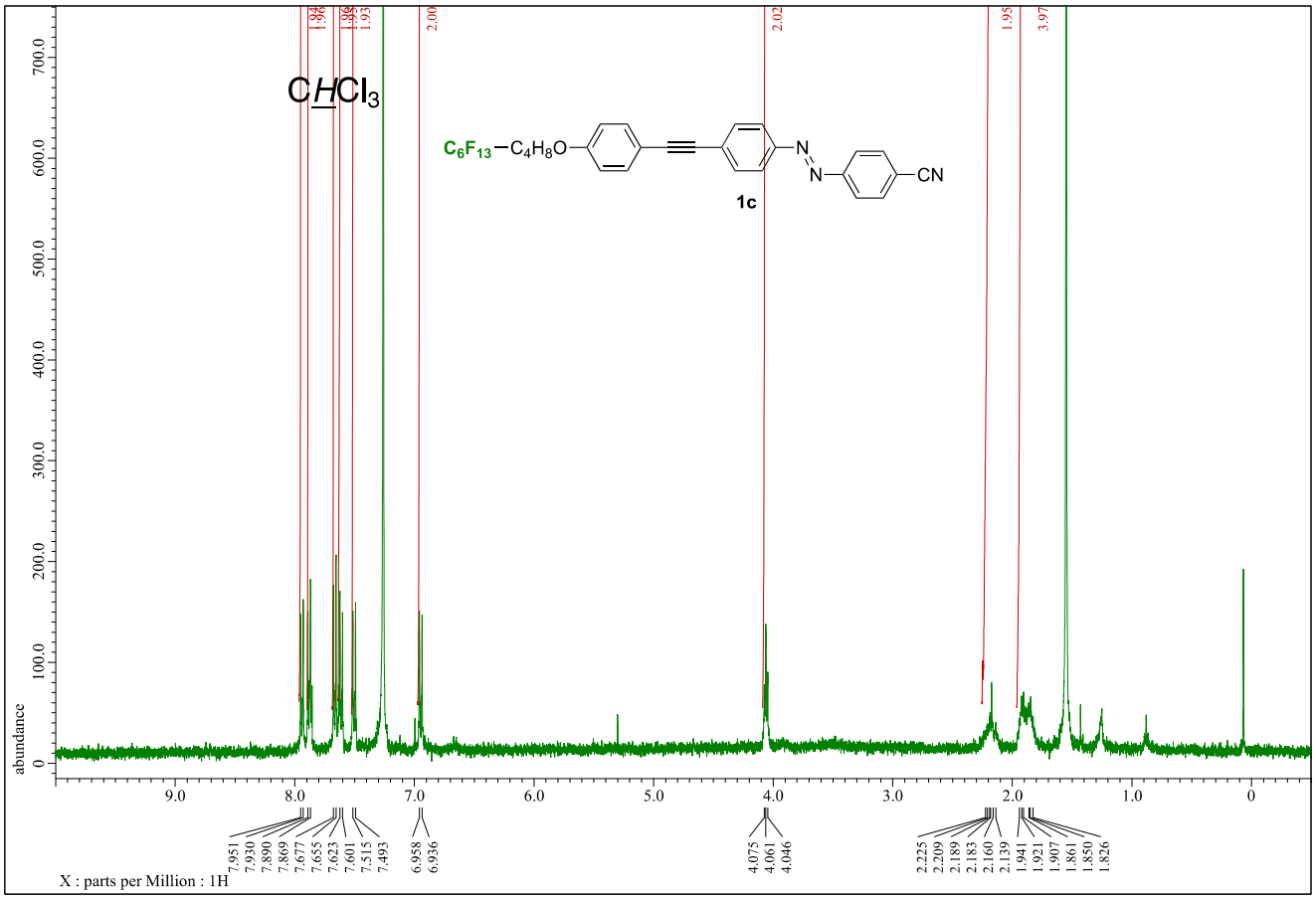

Figure S14. ^{1}H NMR spectrum of **1c** (400 MHz, $CDCl_3$)

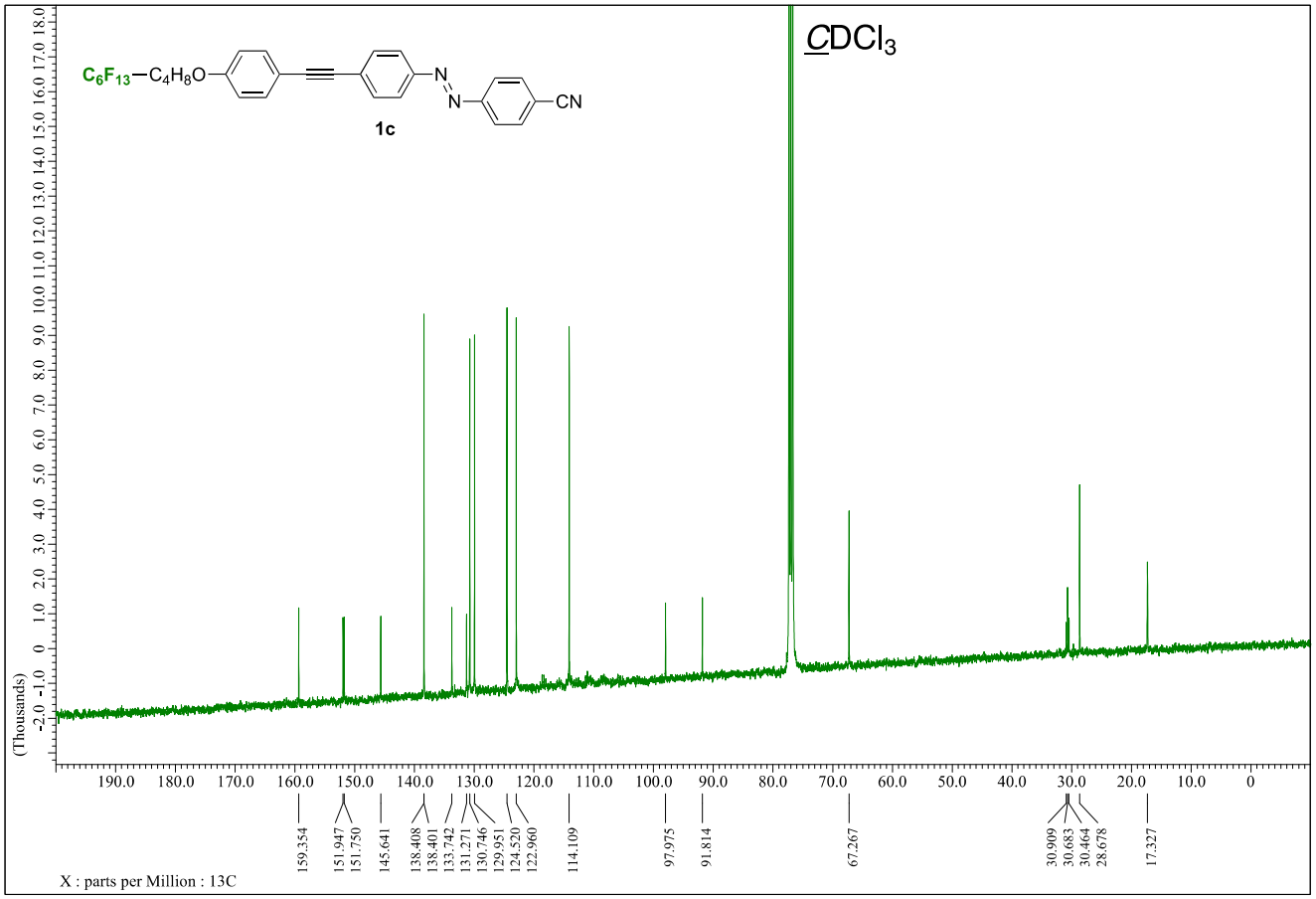

Figure S15. ^{13}C NMR spectrum of **1c** (100 MHz, $CDCl_3$)

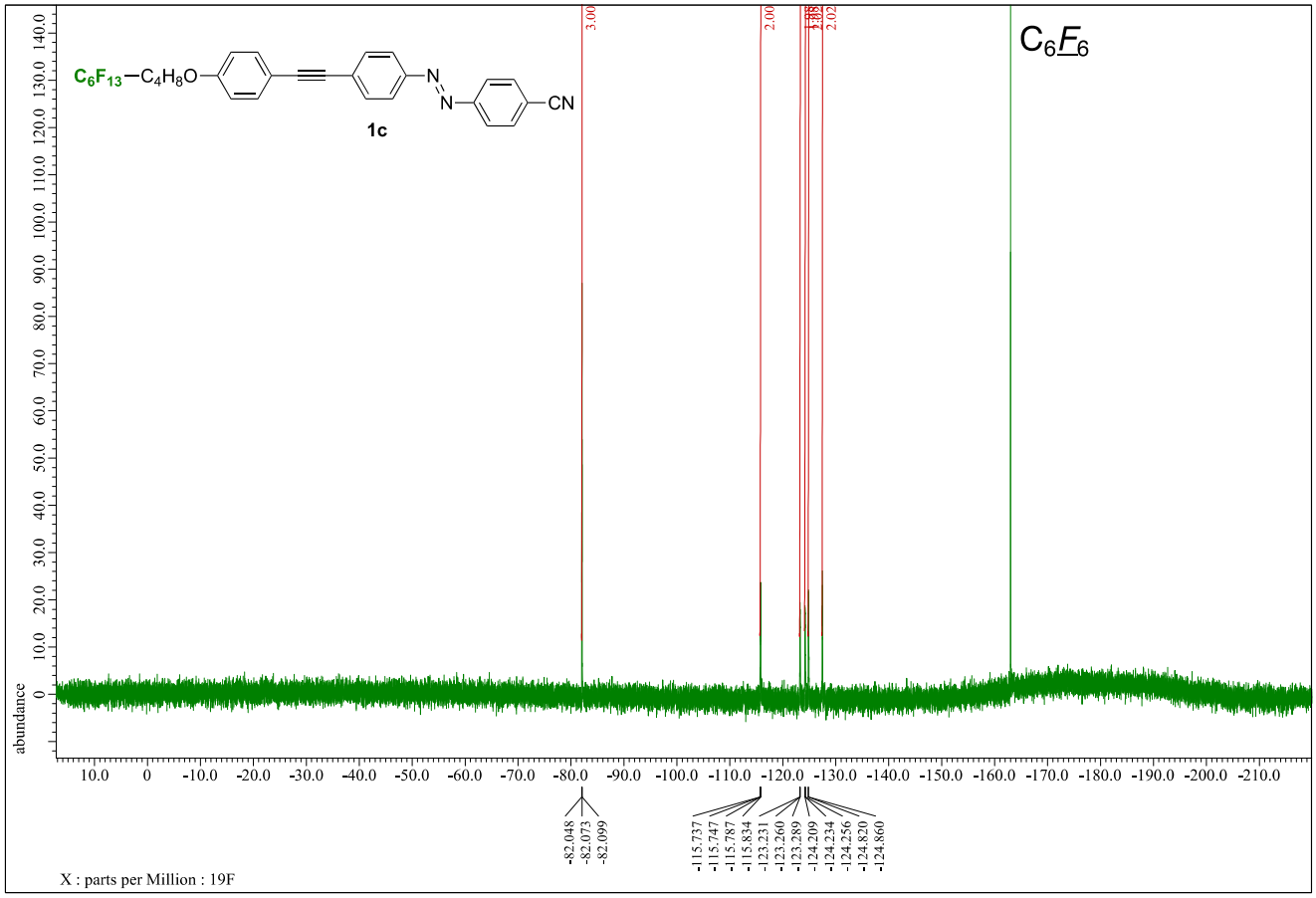

Figure S16. ^{19}F NMR spectrum of **1c** (376 MHz, $CDCl_3$, C_6F_6)

Phase transition behavior

The phase transition behaviors were observed via polarizing optical microscopy (POM) using a BX53 microscope (Olympus, Tokyo, Japan) equipped with a heating and cooling stage (10.002 L, Linkam Scientific Instruments, Redhill, UK). The phase sequences and transition enthalpies were determined using DSC (Shimadzu DSC-60 Plus) at heating and cooling rates of 5.0 °C min^{-1} under an N_2 atmosphere.

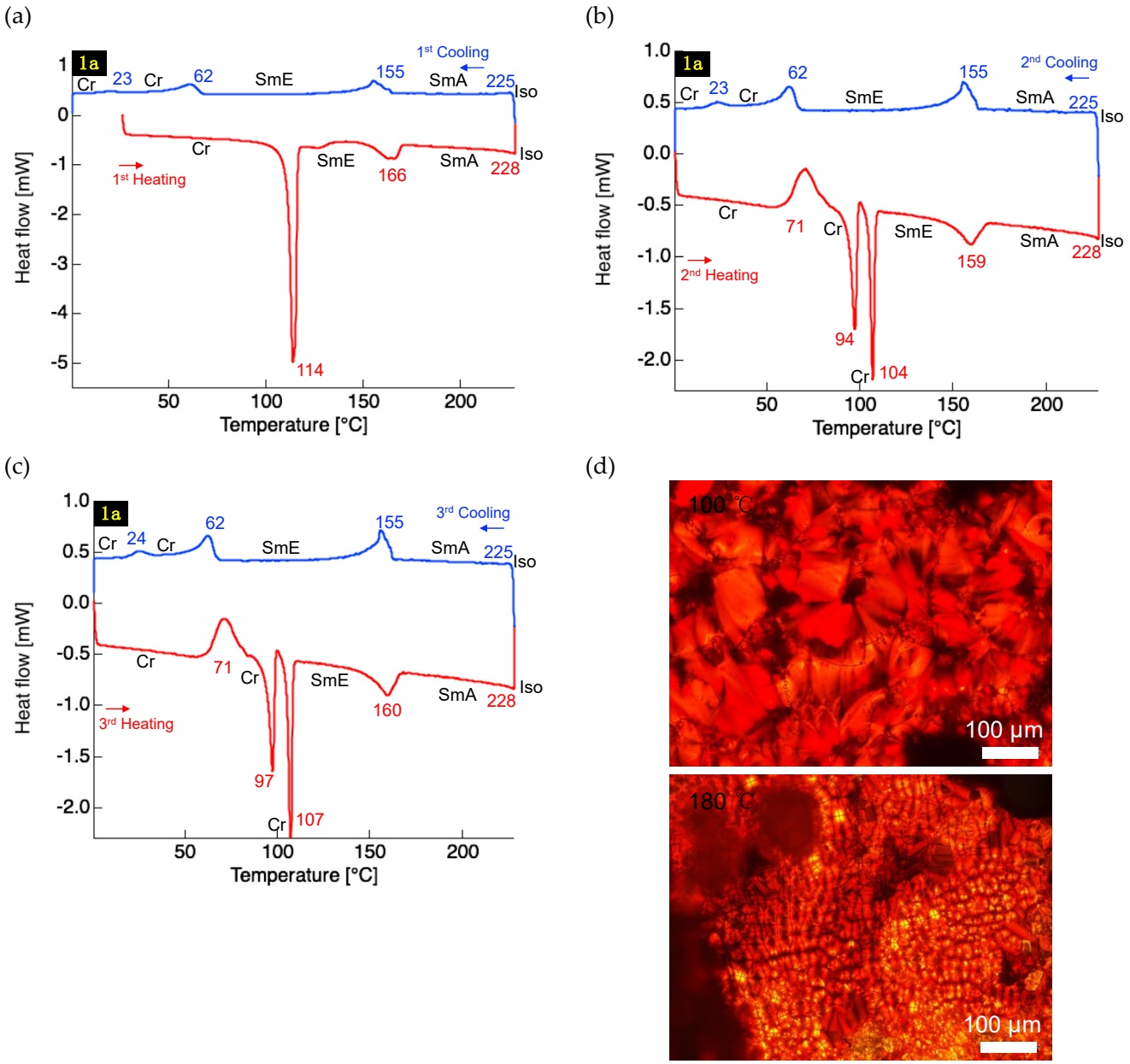

Figure S17. DSC thermograms of **1a** on (a) the 1st heating and cooling cycle, (b) the 2nd cycle and (c) 3rd cycle. (d) POM texture image of **1a** in the mesophase during the cooling process.

Table S1. Phase transition data of **1a**.

Process	Phase transition [1]	Temperature [°C] [2]	DH [kJ mol^{-1}] [2]	DS [J mol^{-1} K^{-1}] [2]
1st Heating	Cr-SmE	114	33.70	87.08
	SmE-SmA	166	6.32	14.41
	SmA-Iso	228 [1]	–	–
1st Cooling	Iso-SmA	225 [1]	–	–
	SmA-SmE	155	–5.87	–13.71
	SmE-Cr	62	–4.89	–14.61
	Cr-Cr	20	–0.56	–1.93
2nd Heating	Cr-Cr	71	–9.46	–27.50
	Cr-Cr	97	9.11	24.61
	Cr-SmE	107	8.08	21.26
	SmE-SmA	160	4.87	11.25
	SmA-Iso	228 [1]	–	–
2nd Cooling	Iso-SmA	225 [1]	–	–
	SmA-SmE	155	–6.25	–14.60
	SmE-Cr	62	–4.18	–12.48
	Cr-Cr	23	–0.64	–2.16
3rd Heating	Cr-Cr	71	–8.39	–24.37
	Cr-Cr	97	8.42	22.73
	Cr-SmE	107	8.74	22.99
	SmE-SmA	160	5.40	12.46
	SmA-Iso	228 [1]	–	–
2nd Cooling	Iso-SmA	224 [1]	–	–
	SmA-SmE	155	–6.21	–14.48
	SmE-Cr	62	–4.49	–13.37
	Cr-Cr	24	–0.73	–2.46

[1] Determined by POM. [2] Determined by DSC.

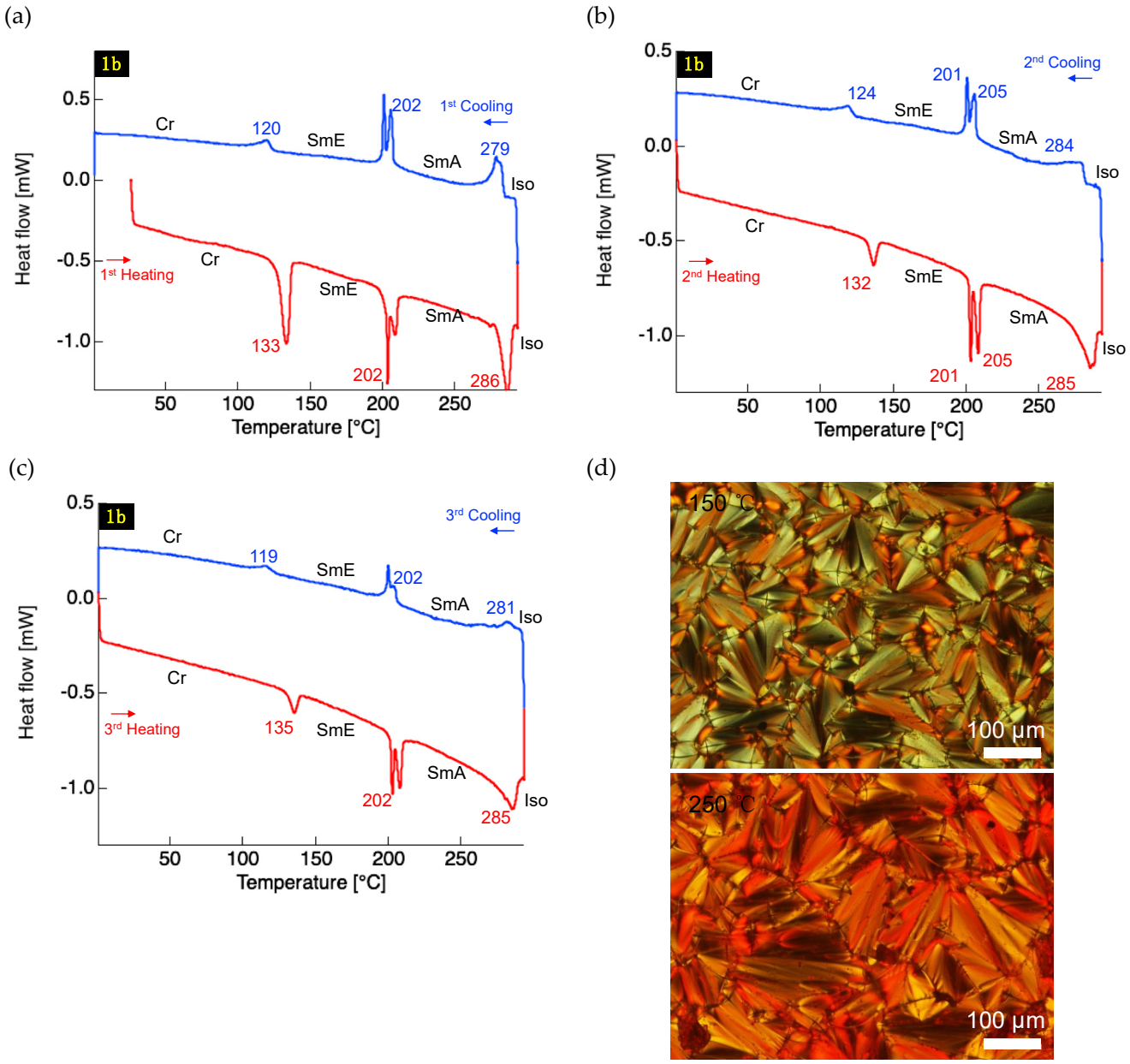

Figure S18. DSC thermograms of **1b** on (a) the 1st heating and cooling cycle, (b) the 2nd cycle and (c) 3rd cycle. (d) POM texture image of **1b** in the mesophase during the cooling process.

Table S2. Phase transition data of **1b**.

Process	Phase transition [1]	Temperature [°C] [2]	DH [kJ mol^{-1}] [2]	DS [J mol^{-1} K^{-1}] [2]
1st Heating	Cr-SmE	133	11.70	28.78
	SmE-SmA	202	7.71	16.20
	SmA-Iso	286	8.99	16.06
1st Cooling	Iso-SmA	279	–7.96	–14.43
	SmA-SmE	202	–6.76	–14.23
	SmE-Cr	120	–2.13	–5.42
2nd Heating	Cr-SmE	136	2.18	5.32
	SmE-SmA	202	6.64	13.99
	SmA-Iso	286	7.23	12.95
2nd Cooling	Iso-SmA	281	–4.97	–8.96
	SmA-SmE	202	–5.28	–11.12
	SmE-Cr	119	–1.86	–4.69
3rd Heating	Cr-SmE	135	1.84	4.50
	SmE-SmA	202	5.89	12.40
	SmA-Iso	285	5.71	10.23
3rd Cooling	Iso-SmA	281	–0.48	–0.86
	SmA-SmE	202	–2.89	–6.09
	SmE-Cr	119	–1.14	–2.92

[1] Determined by POM. [2] Determined by DSC.

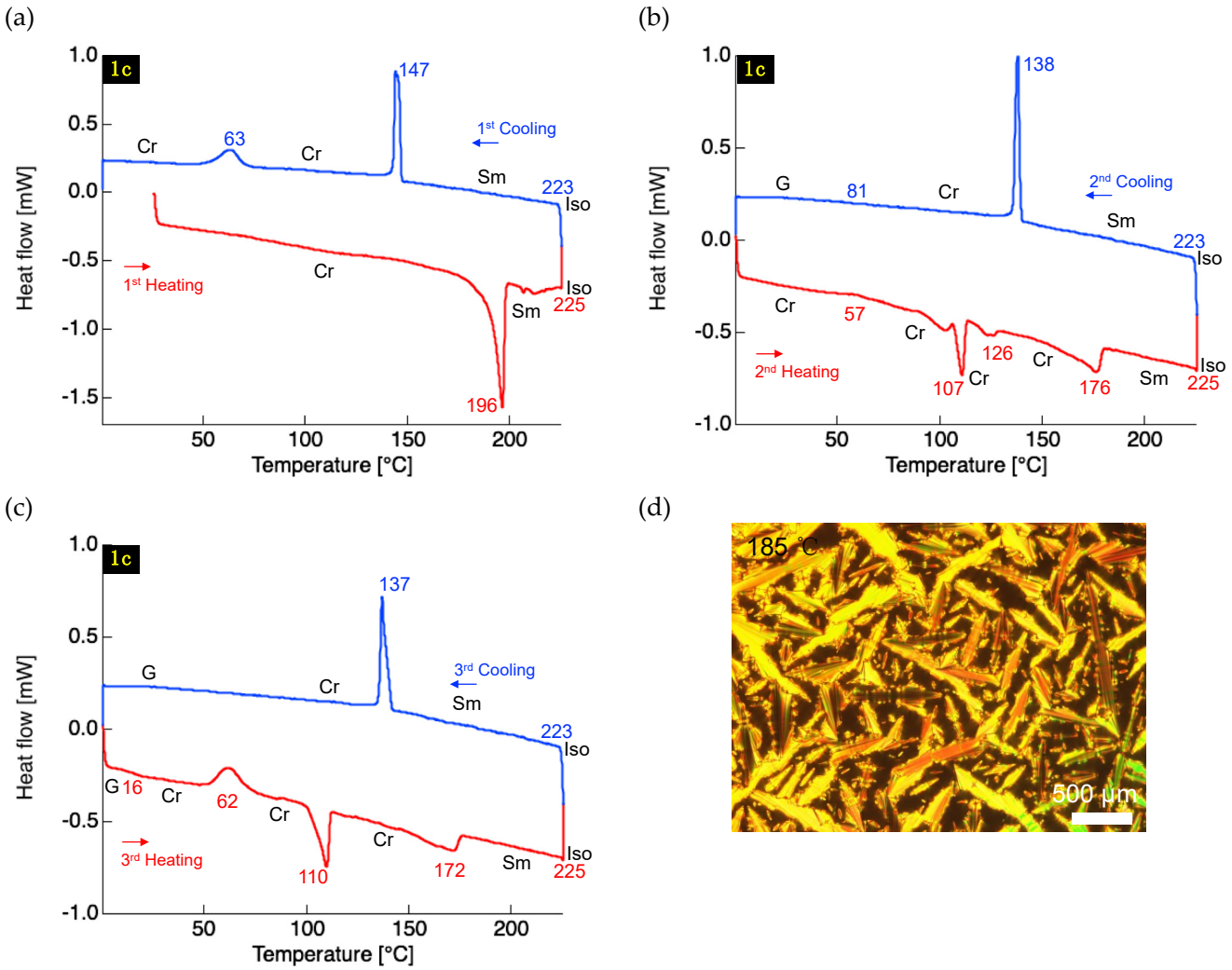

Figure S19. DSC thermograms of **1c** on (a) the 1st heating and cooling cycle, (b) the 2nd cycle and (c) 3rd cycle. (d) POM texture image of **1c** in the mesophase during the cooling process.

Table S3. Phase transition data of **1c**.

Process	Phase transition [1]	Temperature [°C] [2]	DH [kJ mol^{-1}] [2]	DS [J mol^{-1} K^{-1}] [2]
1st Heating	Cr-Sm	196	26.28	55.99
	Sm-Iso	225	– [1]	– [1]
1st Cooling	Iso-Sm	223	– [1]	– [1]
	Sm-Cr	147	–11.70	–27.86
	Cr-Cr	63	–6.41	–19.08
2nd Heating	Cr-Cr	57	–2.22	–6.72
	Cr-Cr	107	8.62	22.70
	Cr-Cr	126	1.60	4.02
	Cr-Sm	176	10.94	24.36
	Sm-Iso	225	– [1]	– [1]
2nd Cooling	Iso-Sm	223	– [1]	– [1]
	Sm-Iso	138	–10.32	–25.11
	Iso-G	81	– [1]	– [1]
3rd Heating	G-Cr	16	– [1]	– [1]
	Cr-Cr	62	–6.84	–20.44
	Cr-Cr	110	8.50	22.21
	Cr-Sm	172	6.70	15.06
	Sm-Iso	225	– [1]	– [1]
3rd Cooling	Iso-Sm	223	– [1]	– [1]
	Sm-Cr	137	–9.29	–22.66
	Cr-G	–	– [1]	– [1]

[1] Determined by POM. [2] Determined by DSC.

Powder X-ray diffraction

The LC structures were evaluated using an FR-E X-ray diffractometer equipped with an R-axis IV 2D detector (Rigaku), and 0.3 mm collimated Cu *K*a radiation (λ = 1.54187 Å) was used as an X-ray beam, with the camera length set at 300 mm. The sample powder was loaded into a thin-walled glass capillary tube (*f* 1.0–2.5 mm) for use in X-ray diffraction (XRD) and annealed up to its isotropic temperature under vacuum. The glass capillary was set on a ceramic heater attached to the FR-E sample holder, and the exposure time of the X-ray beam was 5 min.

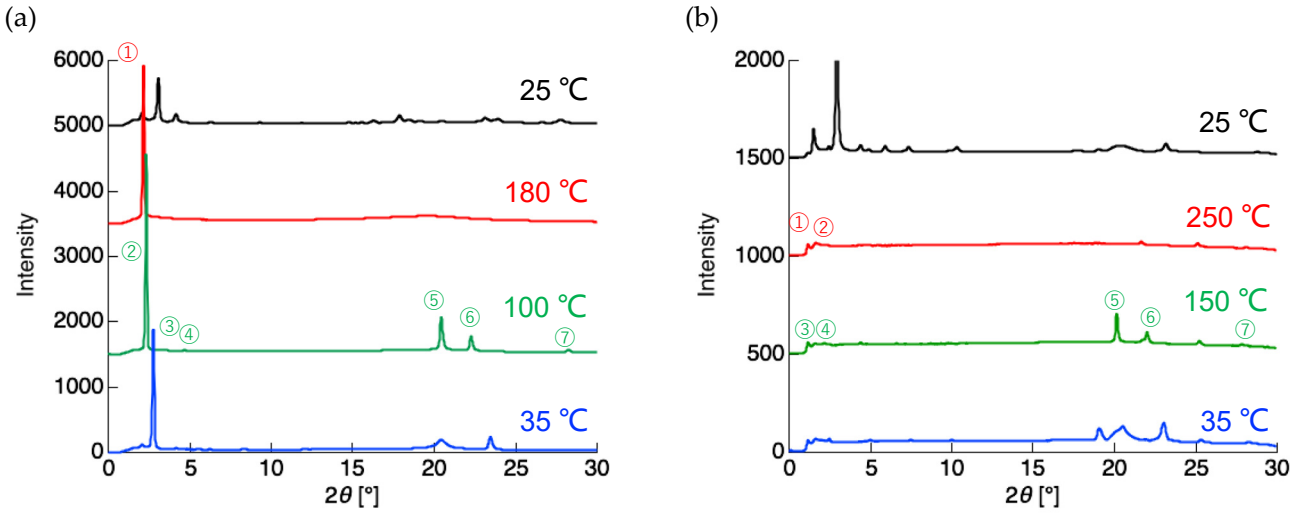

Figure S20. PXRD pattens of (a) **1a** at 25 °C (Cr), 180 °C (SmA), 100 °C (SmE), and 35 °C (Cr), and (b) 1b at 25 °C (Cr), 250 °C (SmA), 150 °C (SmE), and 35 °C (Cr).

Table S4. X-ray diffraction data of **1a** (180 °C and 100 °C) and **1b** (250 °C and 150 °C)

1a				**1b**			
label	2q /°	d /nm	*hkl* index	label	2q /°	d /nm	*hkl* index
1	2.17	4.07	001	1	2.22	3.97	001
2	2.34	3.77	001	2	4.38	2.01	002
3	4.68	1.89	002	3	2.18	4.05	001
4	7.04	1.25	003	4	4.42	2.00	002
5	20.44	0.43	110	5	20.14	0.44	110
6	22.28	0.40	200	6	22.00	0.40	200
7	28.23	0.32	210	7	27.83	0.32	210

Photophysical behavior

Ultraviolet-visible light absorption spectroscopy was performed using a V-750 absorption spectrometer (JASCO, Tokyo, Japan). For the measurement of the solution sample, the transmission method was used, and the samples were prepared by dissolving the compounds in CH_2Cl_2 and adjusting the concentration to 1.0×10^{-5} mol L^{-1}. For the measurement of powder samples, diffuse reflection method was used, and the samples were used pristine crystalline powder obtained by recrystallization.

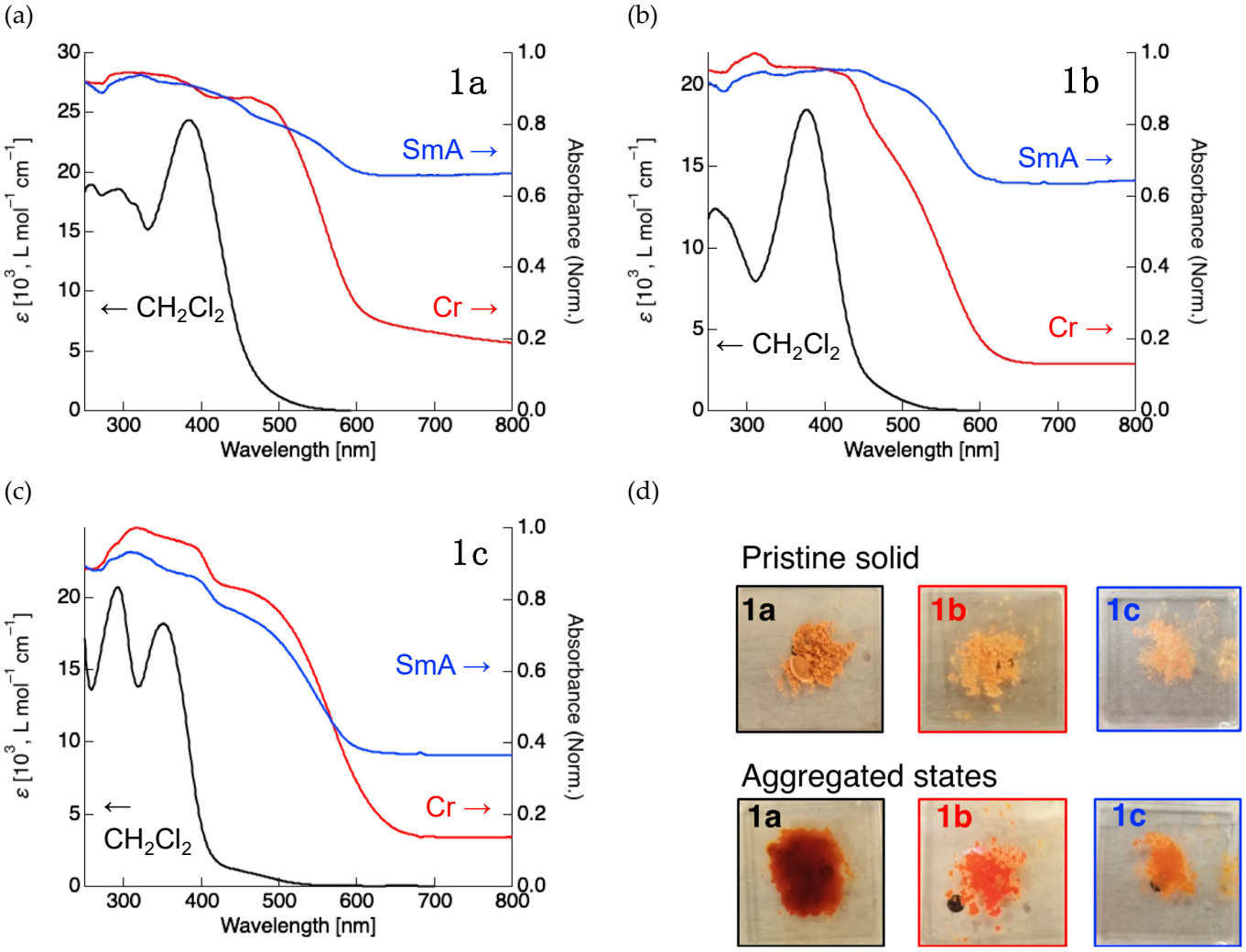

Figure S21. UV-vis Absorption (1.0×10^{-5} mol L^{-1} CH_2Cl_2 solution) and diffuse reflection spectra (pristine solid and aggregated states in SmA phase) of (a) **1a**, (b) **1b**, and (c) **1c**. (d) Photographs of 1a–c in the pristine solid and aggregated states in SmA phase.

(a) (b)

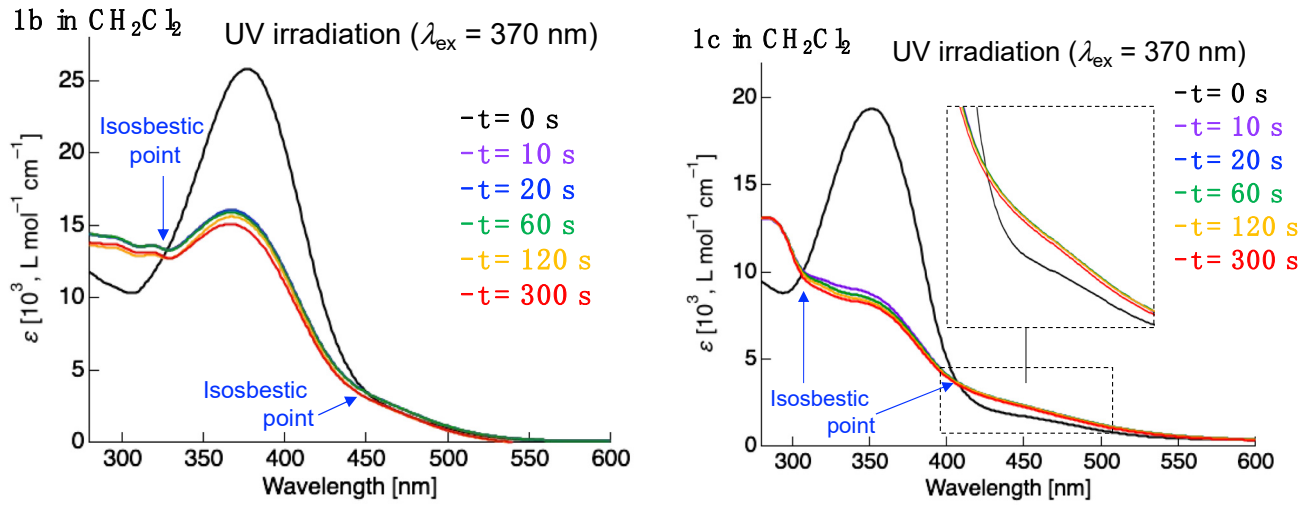

Figure S22. UV-vis. absorption spectral change by UV irradiation of (a) **1b** and (b) **1c** in CH_2Cl_2 solution. Concentration: 1.0×10^{-5} mol L^{-1}.

(a) **1a** (150 °C)

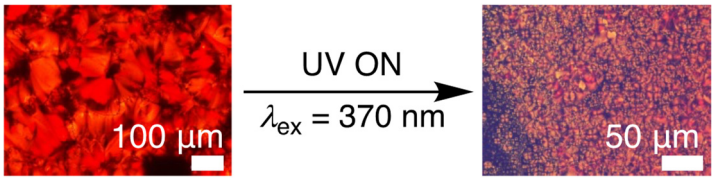

(b) **1b** (180 °C)

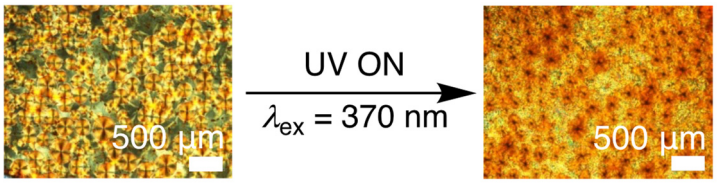

(c) **1c** (190 °C)

Figure S23. POM image change in the mesophase due to UV (l_{ex} = 370 nm) irradiation for (a) **1a** (150 °C), (b) **1b** (180 °C), and (c) **1c** (190 °C).

Theoretical study

Density functional theory (DFT) calculations were conducted using the Gaussian 16 (Rev. B.01) suite of programs (Gaussian, Wallingford, CT, USA), and geometry optimizations were performed at the CAM-B3LYP/6-311+G(d,p)//CAM-B3LYP/6-31+G(d) level of theory with an implicit solvation model, i.e., the conductor-like polarizable continuum model (CPCM), for CH_2Cl_2. Vertical electronic transitions were calculated using time-dependent DFT at the same level of theory.

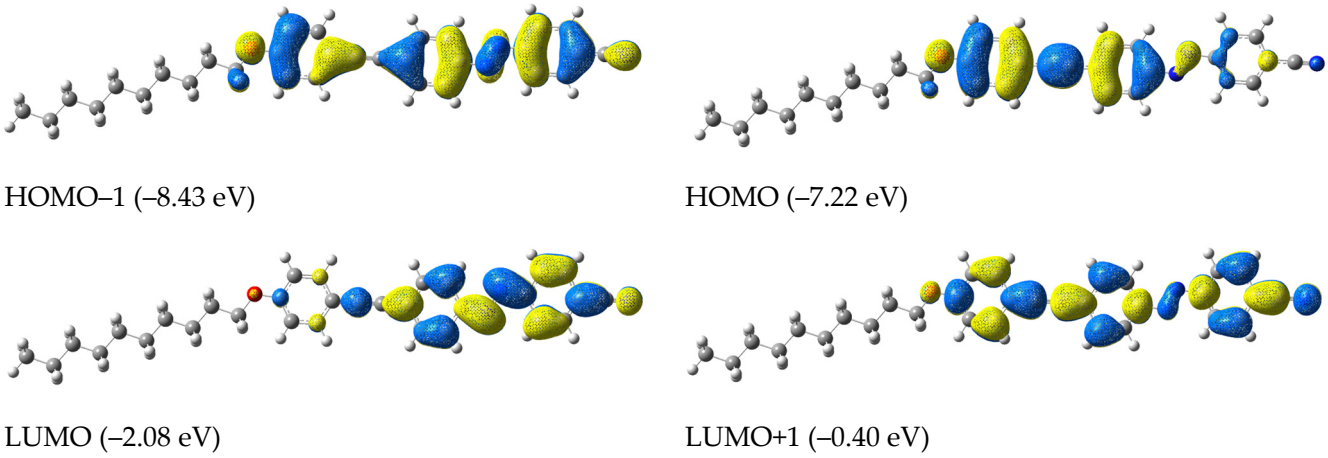

HOMO–1 (–8.43 eV) HOMO (–7.22 eV)

LUMO (–2.08 eV) LUMO+1 (–0.40 eV)

Figure S24. Molecular orbital distributions of HOMO–1, HOMO, LUMO, and LUMO+1 for **1a**.

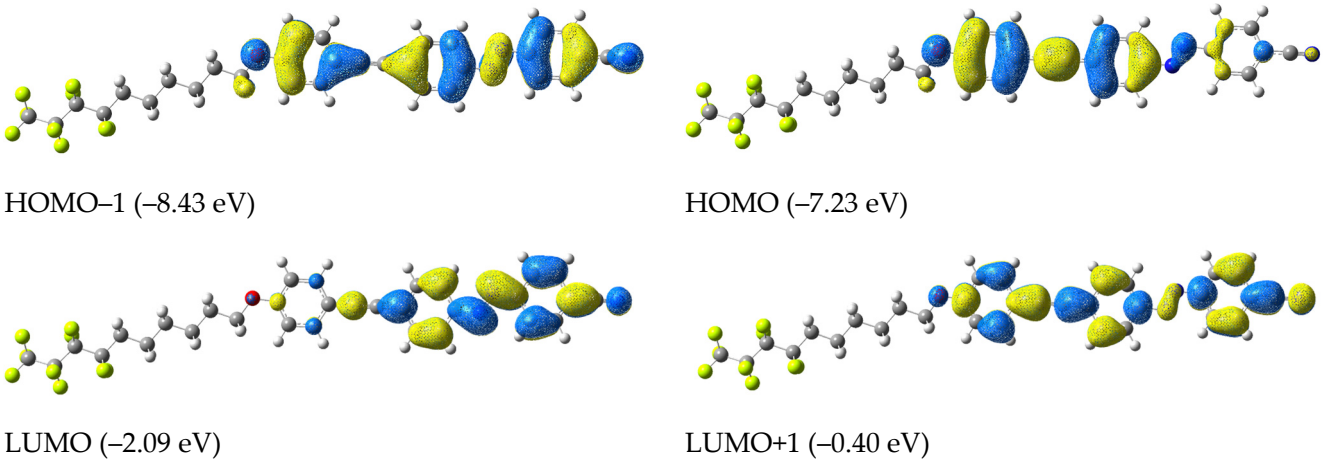

HOMO–1 (–8.43 eV) HOMO (–7.23 eV)

LUMO (–2.09 eV) LUMO+1 (–0.40 eV)

Figure S25. Molecular orbital distributions of HOMO–1, HOMO, LUMO, and LUMO+1 for **1b**.

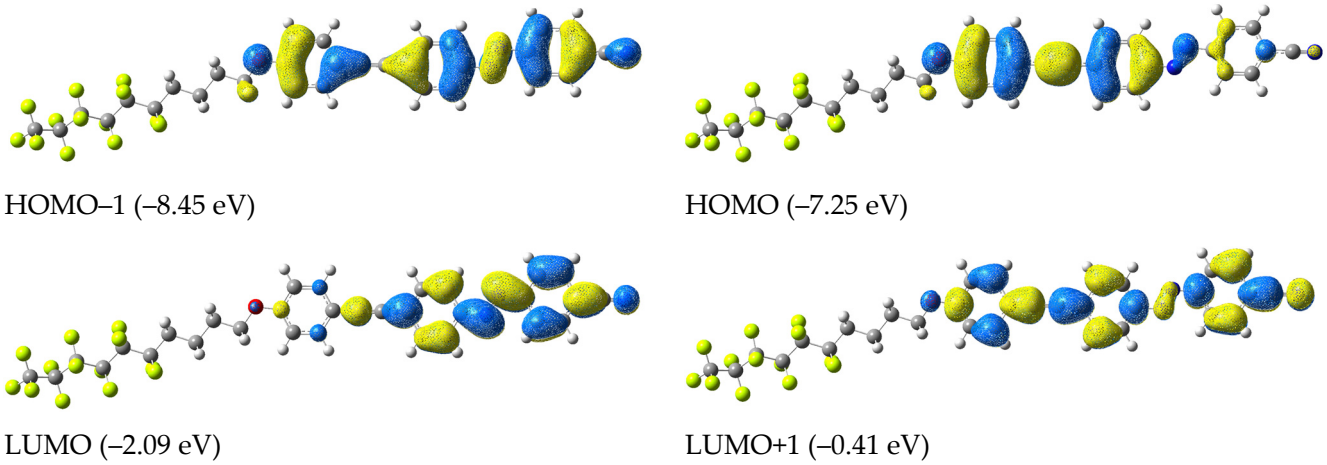

HOMO–1 (–8.45 eV) HOMO (–7.25 eV)

LUMO (–2.09 eV) LUMO+1 (–0.41 eV)

Figure S26. Molecular orbital distributions of HOMO–1, HOMO, LUMO, and LUMO+1 for **1c**.

Table S5. Theoretical electronic transition calculated by TD-DFT method.

Compound	l_{calcd} [nm] [2] (Oscillator strength)	HOMO/LUMO [eV] [2] (DE^{H-L})	Theoretical transition [2] (Contribution)
1a	384 (f = 1.98)	–7.22 eV/ –2.08 eV (5.13 eV)	HOMO → LUMO (78%) HOMO–1 → LUMO (14%) HOMO → LUMO+1 (4%)
1b	384 (f = 1.98)	–7.23 eV/ –2.09 eV (5.14 eV)	HOMO → LUMO (78%) HOMO–1 → LUMO (14%) HOMO → LUMO+1 (4%)
1c	383 (f = 1.98)	–7.25 eV/ –2.09 eV (5.16 eV)	HOMO → LUMO (79%) HOMO–1 → LUMO (14%) HOMO → LUMO+1 (4%)

Table S6. Cartesian coordinates of optimized geometry for **1a**.

No.	Atom No.	Type	Coordinates (Angstroms) x	y	z
1	6	0	10.093453	-0.028173	0.015924
2	6	0	10.973177	1.052663	0.074565
3	6	0	10.583954	-1.337644	-0.041263
4	6	0	12.344003	0.838783	0.079292
5	1	0	10.568556	2.05822	0.116786
6	6	0	11.949928	-1.557636	-0.038006
7	1	0	9.89131	-2.168878	-0.088242
8	6	0	12.832616	-0.469497	0.022839
9	1	0	13.031653	1.675848	0.125849
10	1	0	12.341671	-2.567979	-0.082611
11	7	0	7.933188	-0.662705	-0.00811
12	7	0	8.712307	0.31044	0.016951
13	6	0	14.249051	-0.703064	0.026117
14	7	0	15.391293	-0.892053	0.028809
15	6	0	6.554171	-0.343074	-0.010144
16	6	0	5.684417	-1.434547	-0.024046
17	6	0	6.04155	0.960575	-0.000152
18	6	0	4.31176	-1.236995	-0.026674
19	1	0	6.100842	-2.4367	-0.032277
20	6	0	4.673318	1.158763	-0.003465
21	1	0	6.721069	1.804444	0.009743
22	6	0	3.787922	0.063826	-0.016398
23	1	0	3.637428	-2.086513	-0.036942
24	1	0	4.270282	2.166092	0.003921
25	6	0	2.376457	0.27792	-0.01913
26	6	0	1.178422	0.458509	-0.020941
27	6	0	-0.233999	0.672409	-0.022666
28	6	0	-1.122723	-0.408309	-0.018851
29	6	0	-0.764307	1.975232	-0.027842
30	6	0	-2.499403	-0.210173	-0.019749
31	1	0	-0.731724	-1.42075	-0.014907
32	6	0	-2.130718	2.18096	-0.028966
33	1	0	-0.091058	2.826429	-0.030912
34	6	0	-3.009795	1.090218	-0.024731
35	1	0	-3.156995	-1.07035	-0.016557
36	1	0	-2.543491	3.184578	-0.032884
37	8	0	-4.330695	1.393658	-0.025811
38	6	0	-5.287802	0.332146	-0.018052
39	1	0	-5.140655	-0.29632	-0.905148
40	1	0	-5.136534	-0.286743	0.875072
41	6	0	-6.671776	0.949835	-0.01807
42	1	0	-6.769893	1.600356	0.859575
43	1	0	-6.77578	1.587804	-0.904213
44	6	0	-7.773191	-0.109707	-0.006646
45	1	0	-7.655232	-0.751142	0.877518
46	1	0	-7.660856	-0.764676	-0.881571
47	6	0	-9.17758	0.492663	-0.006718
48	1	0	-9.289547	1.149729	0.867013
49	1	0	-9.296481	1.133564	-0.891466
50	6	0	-10.285712	-0.559142	0.007485
51	1	0	-10.165349	-1.20001	0.892406
52	1	0	-10.172131	-1.216863	-0.865892
53	6	0	-11.691404	0.039958	0.007219
54	1	0	-11.804424	0.698715	0.87994
55	1	0	-11.812059	0.680172	-0.878182
56	6	0	-12.800375	-1.01123	0.023217
57	1	0	-12.679588	-1.651322	0.908765
58	1	0	-12.687157	-1.670238	-0.849362
59	6	0	-14.206408	-0.41317	0.022864
60	1	0	-14.3206	0.246209	0.895178
61	1	0	-14.328572	0.226505	-0.862935
62	6	0	-15.315976	-1.46382	0.039697
63	1	0	-15.194514	-2.102634	0.924842
64	1	0	-15.202464	-2.122425	-0.831895
65	6	0	-16.716732	-0.855111	0.039176
66	1	0	-17.491111	-1.629635	0.051352
67	1	0	-16.869186	-0.216832	0.917452
68	1	0	-16.877146	-0.236692	-0.851799

Table S7. Cartesian coordinates of optimized geometry for **1b**.

No.	Atom No.	Type	Coordinates (Angstroms) x	y	z
1	6	0	-13.497403	-0.132891	0.016286
2	6	0	-14.408253	0.923217	0.039185
3	6	0	-13.94956	-1.457161	-0.002469
4	6	0	-15.772357	0.669652	0.045182
5	1	0	-14.033276	1.941008	0.052541
6	6	0	-15.308512	-1.716767	0.002762
7	1	0	-13.232742	-2.268766	-0.021326
8	6	0	-16.222616	-0.653426	0.026931
9	1	0	-16.484314	1.48731	0.06354
10	1	0	-15.67038	-2.739059	-0.011954
11	7	0	-11.320468	-0.70663	0.0088
12	7	0	-12.126356	0.244794	0.012224
13	6	0	-17.631638	-0.928167	0.032292
14	7	0	-18.767858	-1.150488	0.036645
15	6	0	-9.950756	-0.349591	0.003009
16	6	0	-9.051902	-1.417319	0.006974
17	6	0	-9.473555	0.967401	-0.006673
18	6	0	-7.685132	-1.182807	0.002028
19	1	0	-9.441223	-2.430325	0.014127
20	6	0	-8.111138	1.202469	-0.012056
21	1	0	-10.175794	1.792519	-0.010128
22	6	0	-7.196611	0.131711	-0.007641
23	1	0	-6.987989	-2.013778	0.005315
24	1	0	-7.735494	2.22034	-0.01978
25	6	0	-5.791213	0.382596	-0.013277
26	6	0	-4.59781	0.591456	-0.018084
27	6	0	-3.190592	0.83731	-0.024009
28	6	0	-2.278172	-0.223252	-0.002709
29	6	0	-2.68939	2.151283	-0.051399
30	6	0	-0.906237	0.005325	-0.008319
31	1	0	-2.646615	-1.243899	0.018641
32	6	0	-1.327797	2.387201	-0.057391
33	1	0	-3.38134	2.987183	-0.068081
34	6	0	-0.424999	1.31638	-0.035957
35	1	0	-0.229786	-0.839917	0.008788
36	1	0	-0.93742	3.399531	-0.078591
37	8	0	0.889307	1.64876	-0.04421
38	6	0	1.868311	0.608488	-0.020389
39	1	0	1.733628	0.002941	0.884474
40	1	0	1.732488	-0.039328	-0.895249
41	6	0	3.238606	1.256111	-0.037035
42	1	0	3.327284	1.876384	-0.937161
43	1	0	3.324867	1.927063	0.826192
44	6	0	4.360359	0.218782	-0.005459
45	1	0	4.256232	-0.461013	-0.861868
46	1	0	4.26242	-0.40017	0.896562
47	6	0	5.750446	0.85209	-0.0329
48	1	0	5.852508	1.466325	-0.937524
49	1	0	5.856623	1.534727	0.82084
50	6	0	6.869887	-0.187544	0.005442
51	1	0	6.766794	-0.867491	-0.847876
52	1	0	6.774224	-0.794747	0.912272
53	6	0	8.250293	0.47216	-0.029321
54	1	0	8.361995	1.078235	-0.932825
55	1	0	8.379443	1.137649	0.830641
56	6	0	9.374623	-0.535308	-0.006257
57	6	0	10.788619	0.10024	0.026709
58	6	0	11.977818	-0.870583	-0.218235
59	6	0	13.368142	-0.311696	0.191683
60	9	0	14.315157	-1.136085	-0.261923
61	9	0	13.477954	-0.23086	1.517819
62	9	0	13.56685	0.899134	-0.335589
63	9	0	11.791832	-2.0148	0.470654
64	9	0	10.855532	1.063237	-0.922177
65	9	0	9.277635	-1.347321	1.08767
66	9	0	12.034893	-1.161558	-1.533053
67	9	0	9.326545	-1.351064	-1.104283
68	9	0	10.956647	0.690353	1.234772

Table S8. Cartesian coordinates of optimized geometry for **1c**.

No.	Atom No.	Type	Coordinates (Angstroms) x	y	z
1	6	0	-14.204774	-0.108406	-0.025221
2	6	0	-15.108159	0.953852	0.007068
3	6	0	-14.666234	-1.428824	-0.070383
4	6	0	-16.474046	0.710331	-0.004246
5	1	0	-14.725925	1.968447	0.041254
6	6	0	-16.027027	-1.678405	-0.082342
7	1	0	-13.955197	-2.24532	-0.095886
8	6	0	-16.933625	-0.608899	-0.049066
9	1	0	-17.180201	1.532814	0.021161
10	1	0	-16.396141	-2.697599	-0.117494
11	7	0	-12.031767	-0.697317	-0.02773
12	7	0	-12.831129	0.259402	-0.009904
13	6	0	-18.344589	-0.873286	-0.061574
14	7	0	-19.482379	-1.087223	-0.07168
15	6	0	-10.659621	-0.349621	-0.014162
16	6	0	-9.767955	-1.423249	-0.028716
17	6	0	-10.173677	0.963943	0.011556
18	6	0	-8.399636	-1.198029	-0.017531
19	1	0	-10.164034	-2.43345	-0.048837
20	6	0	-8.809728	1.189747	0.022431
21	1	0	-10.870336	1.793707	0.022455
22	6	0	-7.902431	0.112971	0.008104
23	1	0	-7.708093	-2.033592	-0.028823
24	1	0	-8.427267	2.204908	0.042095
25	6	0	-6.495419	0.354742	0.018945
26	6	0	-5.300902	0.556749	0.027402
27	6	0	-3.892451	0.7957	01c36324
28	6	0	-2.985101	-0.269333	0.030701
29	6	0	-3.385371	2.107578	0.050176
30	6	0	-1.612077	-0.046993	0.037979
31	1	0	-3.358202	-1.288423	0.020317
32	6	0	-2.022695	2.337337	0.057315
33	1	0	-4.07348	2.946762	0.054926
34	6	0	-1.12554	1.261995	0.050878
35	1	0	-0.939576	-0.8956	0.033395
36	1	0	-1.627561	3.347965	0.067616
37	8	0	0.191039	1.588876	0.057714
38	6	0	1.163874	0.544932	0.048746
39	1	0	1.029581	-0.088267	0.934408
40	1	0	1.027618	-0.074791	-0.846053
41	6	0	2.534384	1.193674	0.051626
42	1	0	2.621612	1.843061	-0.827331
43	1	0	2.623194	1.833505	0.937313
44	6	0	3.64967	0.148776	0.044633
45	1	0	3.547243	-0.496169	-0.834557
46	1	0	3.560025	-0.493674	0.927658
47	6	0	5.02701	0.814931	0.034219
48	1	0	5.147409	1.433118	-0.861417
49	1	0	5.143419	1.468593	0.902995
50	6	0	6.152856	-0.191626	0.05861
51	6	0	7.563842	0.444918	-0.044521
52	6	0	8.758408	-0.506494	0.2626
53	6	0	10.128891	0.018959	-0.264436
54	6	0	11.358969	-0.661043	0.40478
55	6	0	12.695998	-0.471015	-0.363917
56	9	0	13.698198	-0.894927	0.407293
57	9	0	12.890935	0.81755	-0.653924
58	9	0	12.699798	-1.177563	-1.493246
59	9	0	11.521754	-0.144646	1.636581
60	9	0	10.1874	-0.197822	-1.594138
61	9	0	8.846844	-0.662899	1.600311
62	9	0	11.137707	-1.986941	0.51065
63	9	0	8.53324	-1.710221	-0.299048
64	9	0	10.214043	1.34535	-0.037868
65	9	0	7.634964	1.480481	0.822602
66	9	0	7.713023	0.932712	-1.299348
67	9	0	6.126314	-0.928857	1.211296
68	9	0	6.035498	-1.076274	-0.974445